

Systematic search of fully heavy tetraquark states

Hong-Tao An^{1,2,*}, Si-Qiang Luo^{1,2,†}, Zhan-Wei Liu^{1,2,3,‡} and Xiang Liu^{1,2,3,§}

¹*School of Physical Science and Technology, Lanzhou University, Lanzhou 730000, China*

²*Research Center for Hadron and CSR Physics, Lanzhou University
and Institute of Modern Physics of CAS, Lanzhou 730000, China*

³*Lanzhou Center for Theoretical Physics, Lanzhou University, Lanzhou, Gansu 730000, China*

(Dated: August 9, 2022)

In 2020, the LHCb collaboration reported a fully charmed tetraquark state $X(6900)$ in the invariant mass spectrum of J/ψ pairs. This discovery inspires us to further study the properties of the fully heavy tetraquark system. In this work, we study systemically all possible configurations for the ground fully heavy tetraquark states in constituent quark model. According to our calculations, we analyze their binding energies, internal mass contributions, relative lengths between (anti)quarks, and the spatial distribution of four valence (anti)quarks. We find no stable S-wave state exist in fully heavy tetraquark system. We hope that our study will be helpful to explore further for fully heavy tetraquark states.

I. INTRODUCTION

The quark model allows not only traditional mesons and baryons, but also exotic states including tetraquarks and pentaquarks. Searching for exotic hadronic states becomes an interesting topic with full of challenges and opportunities. Since the $X(3872)$ was firstly reported by the Belle Collaboration in 2003 [1–3], a series of charmonium-like or bottomonium-like exotic states [4–17] and P_c states [18–20] have been observed in experiment. The various interpretations also have emerged including conventional hadrons, compact tetraquarks or pentaquarks, loosely bound molecules, hybrids, glueballs, kinematic effects and so on.

In 2003, another important observation is that BaBar Collaboration observed a narrow heavy-light state $D_{s0}^*(2317)$ in the $D_s^+\pi^0$ invariant mass spectrum [21]. Its tetraquark with $Qq\bar{q}\bar{q}$ configuration was proposed in Refs.[22–24]. Later, CLEO collaboration [25] confirmed the $D_{s0}^*(2317)$ and observed another narrow resonance $D_{s1}(2460)$ in $D_s^+\pi^0$ final states. The masses of $D_{s0}^*(2317)$ and $D_{s1}(2460)$ deviate from quark model expectations [26] and their decay behaviors are unlike the conventional charmed mesons. Later, SELEX Collaboration reported a charmed-strange meson $D_{sJ}^+(2632)$ in invariant mass spectra of $D_s^+\eta$ and D^0K^+ [27]. In 2016, D0 Collaboration reported a narrow structure $X(5568)$ in the $B_s^0\pi^\pm$ invariant mass spectrum with 5.1σ significance [28]. In 2020, LHCb collaboration reported the discovery of two new exotic structures $X_0(2900)$ and $X_1(2900)$ [29, 30], which reignites the study of exotic charmed mesons [31–40].

In 2017, the LHCb Collaboration reported the observation of Ξ_{cc}^{++} in the $\Lambda_c^+K^-\pi^+\pi^+$ decay mode and its mass was determined to be $3621.40 \pm 0.72(stat.) \pm 0.27(syst.) \pm$

$0.14(\Lambda_c^+)$ MeV [42]. This observation motivates theorists to further study the possible stable tetraquark states with $QQ\bar{q}\bar{q}$ configuration [43–51]. Recently, the LHCb Collaboration discovered a very narrow state, called T_{cc}^+ by analyzing the $D^0D^0\pi^+$ invariant mass spectrum, which has a minimal quark configuration of $cc\bar{u}\bar{d}$ [52]. To our knowledge, the tetraquark states with $QQ\bar{Q}\bar{q}$ configurations are also studied in different frames [53–57].

As for the tetraquark state with $QQ\bar{Q}\bar{Q}$ configuration, it has inspired both the experimental and theoretical attention. The existence of four heavy quark states was discussed in a specific potential models [58]. The $Q^2\bar{Q}^2$ system was studied with the Born-Oppenheimer approximation in the MIT bag model [59]. Moreover, Lloyd et al. investigated four-body states with only charmed quarks ($cc\bar{c}\bar{c}$) in a parameterized non-relativistic Hamiltonian [60]. Working in a large but finite oscillator basis, they found several close-lying bound states. Later, Karliner et al. estimated masses of $Q_1Q_2\bar{Q}_3\bar{Q}_4$ resonant states in a simple quark model, suggested how to produce and observe them, and obtained $M(X_{cc\bar{c}\bar{c}}) = 6192 \pm 25$ MeV and $M(X_{bb\bar{b}\bar{b}}) = 18826 \pm 25$ MeV for the $J^{PC} = 0^{++}$ states involving charmed and bottom tetraquarks [61]. Anwar et al. calculated the ground-state energy of the $bb\bar{b}\bar{b}$ bound state in a nonrelativistic effective field theory with one-gluon-exchange (OGE) color Coulomb interaction, and the ground state $bb\bar{b}\bar{b}$ tetraquark mass is predicted to be (18.72 ± 0.02) GeV [62]. In 2016, Bai et al. presented a calculation of the $bb\bar{b}\bar{b}$ tetraquark ground-state energy using a diffusion Monte Carlo method to solve the non-relativistic many-body system [63]. In 2017, Debastiani et al. extended updated Cornell model to study the all-charm tetraquark ($c\bar{c}c\bar{c}$) in a diquark-antidiquark configuration [64]. Moreover, Chen et al. used a moment QCD sum rule method augmented by fundamental inequalities to research the existence of exotic states $cc\bar{c}\bar{c}$ and $bb\bar{b}\bar{b}$ in the compact diquark-antidiquark configuration. Meanwhile, they suggested to search for the doubly hidden-charm states in the $J/\psi J/\psi$ and $\eta_c(1S)\eta_{1S}$ channels [65].

In 2016, the CMS Collaboration reported the first ob-

* anht14@lzu.edu.cn

† luosq15@lzu.edu.cn

‡ liuzhanwei@lzu.edu.cn

§ xiangliu@lzu.edu.cn

ervation of the $\Upsilon(1S)$ pair production in pp collisions and they found an exotic structure in four lepton channel around 18.4 GeV with a global significance of 3.6σ , which is probably a fully-bottom tetraquark state [66]. However, such a structure was not confirmed by latter CMS experiments [67]. After that, the LHCb Collaboration studied the $\Upsilon(1S)_{\mu^+\mu^-}$ invariant mass distribution to seek a possible $bb\bar{b}\bar{b}$ exotic meson, but they did not see any significant excess in the range 17.5 – 20.0 GeV [68].

In 2020, the LHCb Collaboration declared a narrow resonance X(6900) in the di- J/ψ mass spectrum with the significance more than 5σ [69]. Moreover, a broad structure ranging from 6.2 to 6.8 GeV and an underlying peak near 7.3 GeV was also reported at the same time [69]. Recently, the ATLAS and CMS collaborations released their measurements on di- J/ψ invariant mass spectrum. They both confirmed the existence of the X(6900), meanwhile they also found the signals of some new peaking structures [70, 71]. These structures could be expected widely to be a $cc\bar{c}\bar{c}$ configuration. The observation of X(6900) attracts many scholars to interpret this state from different views: (1) the first radial excitation states of $0^{++}/2^{++}$ or the first orbital excitation state of $0^{-+}/1^{-+}$ [72–77]; (2) a bound diquark-antidiquark system [78–80]; (3) the gluonic tetracharm state in $[\bar{3}_c]_{cc} \otimes [8_c] \otimes [3_c]_{\bar{c}\bar{c}}$ configuration with $J^{PC} = 0^{++}$ [81]; (4) a dynamically generated resonance pole structure due to the coupled-channel interactions between $J/\psi - J/\psi$, $J/\psi - \psi'$, and $\psi' - \psi'$ [82]; (5) a $J^{PC} = 0^{++}$ BSM Higgs-like boson [83]; (6) a non-resonant dynamical mechanism to understand several new structures observed by LHCb [84, 85]; (7) the scalar and axialvector four-quark states [86]; (8) a cusp effect from the $J/\psi\psi(3770)$ channel [87].

For the stability of the fully heavy tetraquark state, it has been discussed for a long time. Debastiani et al. found that the lowest S-wave $cc\bar{c}\bar{c}$ tetraquarks might be below the dicharmonium thresholds in their updated Cornell model [88]. The 1^+ $bb\bar{b}\bar{c}$ state is thought to be a narrow state in the extended chromomagnetic model [89]. However, many other studies suggested that the ground state of fully heavy tetraquarks is above the dimeson threshold. Wang et al. also calculated the fully-heavy tetraquark state in two nonrelativistic quark models, which have different OGE Coulomb, linear confinement and hyperfine potentials [90]. Based on the numerical calculations, they thought their ground states are located about 300 – 450 MeV above the lowest scattering states, which indicates that there may not exist bound tetraquark state. The lattice nonrelativistic QCD methodology was adopted to study the lowest energy eigenstate of the $bb\bar{b}\bar{b}$ system, and no state was found below the lowest bottomonium-pair threshold [91]. Moreover, JR Richard et al. also thought the all-heavy configuration $QQ\bar{Q}\bar{Q}$ is not stable if one adopts a standard quark model and solves the four-body problem correctly [92]. Xin Jin et al. investigated full-charm and full-bottom tetraquark by the quark delocalization color screening model and the chiral quark model, re-

spectively, and the results within the quantum numbers $J^P = 0^+, 1^+,$ and 2^+ show that bound state is in existent by both models [93]. Until now, this topic is still an open issue.

Inspired by these, we use the variational method to calculate the ground state masses for fully heavy tetraquark states. Moreover, we also provide the binding energies, the internal mass contributions, the expectation value of the hyperfine potential, the relative distances between (anti)quarks, and the spatial distribution of four valence (anti)quarks for every state.

This paper is organized as followings. Firstly, we introduce the Hamiltonian of the constituent quark model and give the corresponding parameters in Section II. Next we give the spatial function in a simple Gaussian form and construct the flavor, color, and spin wave functions of fully heavy tetraquark states in Section III. Then, we show the numerical results obtained from the variational method and further analyze the internal mass contributions and relative lengths between (anti) quarks in Section IV. Finally, we give a short summary in Section V.

II. HAMILTONIAN

We choose a nonrelativistic Hamiltonian for fully heavy tetraquark system, which is written as,

$$H = \sum_{i=1}^4 \left(m_i + \frac{\mathbf{p}_i^2}{2m_i} \right) - \frac{3}{4} \sum_{i<j} \frac{\lambda_i^c \cdot \lambda_j^c}{2} (V_{ij}^{Con} + V_{ij}^{SS}). \quad (1)$$

Here, m_i is the (anti)quark mass, λ_i^c is the $SU(3)$ color operator for the i -th quark, and for antiquark, λ_i^c is replaced with $-\lambda_i^{c*}$. The internal quark potentials V_{ij}^{Con} and V_{ij}^{SS} have the following forms:

$$\begin{aligned} V_{ij}^{Con} &= -\frac{\kappa}{r_{ij}} + \frac{r_{ij}}{a_0^2} - D, \\ V_{ij}^{SS} &= \frac{\kappa'}{m_i m_j} \frac{1}{r_{0ij} r_{ij}} e^{-r_{ij}^2/r_{0ij}^2} \sigma_i \cdot \sigma_j, \end{aligned} \quad (2)$$

where $r_{ij} = |\mathbf{r}_i - \mathbf{r}_j|$ is the distance between the i -th (anti)quark and the j -th (anti)quark, and the σ_i is the $SU(2)$ spin operator for the i -th quark. As for the r_{0ij} and κ' , we have

$$\begin{aligned} r_{0ij} &= 1/(\alpha + \beta \frac{m_i m_j}{m_i + m_j}), \\ \kappa' &= \kappa_0 (1 + \gamma \frac{m_i m_j}{m_i + m_j}). \end{aligned} \quad (3)$$

The corresponding parameters appearing in Eqs. (2-3) are shown in Table I. Here, κ and κ' are the couplings of the Coulomb and hyperfine potentials, respectively, and they are proportional to the running coupling constant $\alpha_s(r)$ of QCD. The Coulomb and hyperfine interaction can be deduced from the one-gluon-exchange model. $1/a_0^2$ represents the strength of linear potential. r_{0ij} is the Gaussian-smearing parameter. Further, we introduce

κ_0 and γ in κ' to provide better descriptions for the interaction between different quark pairs [94].

TABLE I. Parameters of the Hamiltonian.

Parameter	κ	a_0	D
Value	120.0 MeV fm	0.0318119 (MeV ⁻¹ fm) ^{1/2}	983 MeV
Parameter	α	β	m_c
Value	1.0499 fm ⁻¹	0.0008314 (MeVfm) ⁻¹	1918 MeV
Parameter	κ_0	γ	m_b
Value	194.144 MeV	0.00088 MeV ⁻¹	5343 MeV

III. WAVE FUNCTIONS

Here, we concentrate on the ground fully-heavy tetraquark states. We present the flavor, spatial, and color-spin parts of total wave function for fully-heavy tetraquark system. In order to consider the constraint from the Pauli principle, we use a diquark-antidiquark picture to analyze this tetraquark system.

A. Flavor Part

Firstly, we discuss the flavor part. Here, we list all the possible flavor combinations for the fully-heavy tetraquark system in Table II.

In Table II, the three flavor combinations in the first line are purely neutral particles and the C parity is a ‘‘good’’ quantum number. For the other six states in the second line, every state has a charge conjugation anti-partner, and their masses, internal mass contributions, relative distances between (anti)quarks are absolutely same, and thus we only need to discuss one of the pair.

Moreover, the $cc\bar{c}\bar{c}$, $bb\bar{b}\bar{b}$, and $c\bar{c}b\bar{b}$ states have the two pairs of (anti)quarks which are identical, but only the first two quarks in the $cc\bar{c}\bar{b}$ and $bb\bar{b}\bar{c}$ states are identical.

B. Spatial Part

In this part, we construct the wave function for the spatial part in a simple Gaussian form. We denote the fully heavy tetraquark state as $Q(1)Q(2)\bar{Q}(3)\bar{Q}(4)$ configuration, and choose the Jacobian coordinates system as follows:

$$\begin{aligned} \mathbf{x}_1 &= \sqrt{1/2}(\mathbf{r}_1 - \mathbf{r}_2); \\ \mathbf{x}_2 &= \sqrt{1/2}(\mathbf{r}_3 - \mathbf{r}_4); \\ \mathbf{x}_3 &= \frac{1}{2}[(\frac{m_1\mathbf{r}_1 + m_2\mathbf{r}_2}{m_1 + m_2}) - (\frac{m_3\mathbf{r}_3 + m_4\mathbf{r}_4}{m_3 + m_4})]. \end{aligned} \quad (4)$$

TABLE II. All possible flavor combinations for the fully-heavy tetraquark system.

System	Flavor combinations		
$QQ\bar{Q}\bar{Q}$	$cc\bar{c}\bar{c}$	$bb\bar{b}\bar{b}$	$c\bar{c}b\bar{b}$
	$cc\bar{b}\bar{b}$ ($bb\bar{c}\bar{c}$)	$cc\bar{c}\bar{b}$ ($bc\bar{c}\bar{c}$)	$bb\bar{b}\bar{c}$ ($cb\bar{b}\bar{b}$)

Here, we set the Jacobi coordinates with the following conditions:

$$\begin{aligned} m_1 = m_2 = m_3 = m_4 = m_c, & \quad \text{for } cc\bar{c}\bar{c}, \\ m_1 = m_2 = m_3 = m_4 = m_b, & \quad \text{for } bb\bar{b}\bar{b}, \\ m_1 = m_2 = m_c, m_3 = m_4 = m_b, & \quad \text{for } cc\bar{b}\bar{b}, \\ m_1 = m_2 = m_3 = m_c, m_4 = m_b, & \quad \text{for } cc\bar{c}\bar{b}, \\ m_1 = m_2 = m_3 = m_b, m_4 = m_c, & \quad \text{for } bb\bar{b}\bar{c}, \\ m_1 = m_c, m_2 = m_b, m_3 = m_c, m_4 = m_b, & \quad \text{for } c\bar{c}b\bar{b}. \end{aligned}$$

Based on these, we construct the spatial wave functions of $QQ\bar{Q}\bar{Q}$ states in a single Gaussian form. The spatial wave function can satisfy the required symmetry property:

$$R^s = \exp[-C_{11}\mathbf{x}_1^2 - C_{22}\mathbf{x}_2^2 - C_{33}\mathbf{x}_3^2], \quad (5)$$

where C_{11} , C_{22} , and C_{33} are the variational parameters.

Moreover, it is useful to introduce the center of mass frame so that the kinetic term in the Hamiltonian of Eq. (1) can be reduced appropriately for our calculations. The kinetic term denoted by T_c is as follows:

$$T_c = \sum_{i=1}^4 \frac{\mathbf{P}_i^2}{2m_i} - \frac{\mathbf{P}_{rC}^2}{2M} = \frac{\mathbf{P}_{x_1}^2}{2m'_1} + \frac{\mathbf{P}_{x_2}^2}{2m'_2} + \frac{\mathbf{P}_{x_3}^2}{2m'_3}, \quad (6)$$

where different states have different reduced masses m'_i and we show them in Table III.

TABLE III. The reduced mass m'_i in different states.

States	m'_1	m'_2	m'_3	States	m'_1	m'_2	m'_3
$cc\bar{c}\bar{c}$	m_c	m_c	m_c	$cc\bar{c}\bar{b}$	m_c	$\frac{2m_c m_b}{m_c + m_b}$	$\frac{(m_c + m_b)m_c}{2(3m_c + m_b)}$
$bb\bar{b}\bar{b}$	m_b	m_b	m_b	$bb\bar{b}\bar{c}$	m_b	$\frac{2m_c m_b}{m_c + m_b}$	$\frac{(m_c + m_b)m_b}{2(3m_b + m_c)}$
$cc\bar{b}\bar{b}$	m_c	m_b	$\frac{2m_c m_b}{m_c + m_b}$	$c\bar{c}b\bar{b}$	$\frac{2m_c m_b}{m_c + m_b}$	$\frac{2m_c m_b}{m_c + m_b}$	$\frac{m_c + m_b}{2}$

C. Color-spin Part

In the color space, the color wave functions can be analyzed by applying the SU(3) group theory, where the direct product of the diquark-antidiquark components reads:

$$(3_c \otimes 3_c) \otimes (\bar{3}_c \otimes \bar{3}_c) = (6_c \oplus \bar{3}_c) \otimes (\bar{6}_c \oplus 3_c). \quad (7)$$

Based on these, we get two kinds of color-singlet state:

$$\phi_1 = |(Q_1 Q_2)^3 (\bar{Q}_3 \bar{Q}_4)^3\rangle, \phi_2 = |(Q_1 Q_2)^6 (\bar{Q}_3 \bar{Q}_4)^6\rangle. \quad (8)$$

In the spin space, the allowed wave functions in diquark-antidiquark picture read:

$$\begin{aligned} \chi_1 &= |(Q_1 Q_2)_1 (\bar{Q}_3 \bar{Q}_4)_1\rangle_2, \chi_2 = |(Q_1 Q_2)_1 (\bar{Q}_3 \bar{Q}_4)_1\rangle_1, \\ \chi_3 &= |(Q_1 Q_2)_1 (\bar{Q}_3 \bar{Q}_4)_0\rangle_1, \chi_4 = |(Q_1 Q_2)_0 (\bar{Q}_3 \bar{Q}_4)_1\rangle_1, \\ \chi_5 &= |(Q_1 Q_2)_1 (\bar{Q}_3 \bar{Q}_4)_1\rangle_0, \chi_6 = |(Q_1 Q_2)_0 (\bar{Q}_3 \bar{Q}_4)_0\rangle_0. \end{aligned} \quad (9)$$

In the notation $|(Q_1 Q_2)_{\text{spin}1} (\bar{Q}_3 \bar{Q}_4)_{\text{spin}2}\rangle_{\text{spin}3}$, the spin1, spin2, and spin3 represent the spins of diquark, antidiquark, and the whole tetraquark state, respectively.

Because the flavor part and spatial part are chosen to be fully symmetric for the (anti)diquark, the color-spin part of the total wave function should be fully antisymmetric. Combining the flavor part, we show all possible color-spin part satisfied Pauli principle with J^{PC} in Table IV.

TABLE IV. The allowed color-spin parts for every flavor configuration.

Type	$J^{P(C)}$	Color-spin Part			
$cc\bar{c}\bar{c}$	$2^{+(+)}$	$\phi_1 \chi_1$			
$bb\bar{b}\bar{b}$	$1^{+(-)}$	$\phi_1 \chi_2$			
$cc\bar{b}\bar{b}$	$0^{+(+)}$	$\phi_1 \chi_5$	$\phi_2 \chi_6$		
$cc\bar{c}\bar{b}$	2^+	$\phi_1 \chi_1$			
	1^+	$\phi_1 \chi_2$	$\phi_1 \chi_3$	$\phi_2 \chi_4$	
$bb\bar{b}\bar{c}$	0^+	$\phi_1 \chi_5$	$\phi_2 \chi_6$		
	2^{++}	$\phi_1 \chi_1$	$\phi_2 \chi_1$		
	1^{+-}	$\phi_1 \chi_2$	$\phi_2 \chi_2$	$\frac{1}{\sqrt{2}}(\phi_1 \chi_3 + \phi_1 \chi_4)$	
$cb\bar{c}\bar{b}$		$\frac{1}{\sqrt{2}}(\phi_2 \chi_3 + \phi_2 \chi_4)$			
	1^{++}	$\frac{1}{\sqrt{2}}(\phi_1 \chi_3 - \phi_1 \chi_4)$	$\frac{1}{\sqrt{2}}(\phi_2 \chi_3 - \phi_2 \chi_4)$		
	0^{++}	$\phi_1 \chi_5$	$\phi_2 \chi_5$	$\phi_1 \chi_6$	$\phi_2 \chi_5$

IV. NUMERICAL ANALYSIS

In this section, we firstly introduce a useful method that can be used to examine the stability of the tetraquarks through the eigenvalue of the hyperfine potential matrix generated by the independent color \otimes spin bases. This hyperfine matrix is essential in identifying possible attraction [95–99]. A stable or resonant multi-quark state can only exist if the hyperfine potential of the multi-quark configuration is sufficiently attractive compared to its rearrangement decay channels [99]. Here, the matrix form of the hyperfine factor is given as $\langle \sum_{i < j}^4 -\frac{1}{m_i m_j} \lambda_i^c \cdot \lambda_j^c \sigma_i \cdot \sigma_j \rangle$. Then, we diagonalize them to get the lowest eigenvalue of the hyperfine factor, and

show them in corresponding Tables. To compare the expectation values of the tetraquarks' hyperfine factor better, we also show the corresponding values for all possible decay channels in same Tables.

Next, we check the consistence between the experimental masses and the obtained masses of some mesons using the variational method based on the Hamiltonian of Eq. 1 and the parameters in Table I. We show the results in Table V and notice that our values are relatively reliable since the deviations for most states are less than 10 MeV.

TABLE V. Masses of some mesons obtained from the theoretical calculations. The masses and errors are in units of MeV. The variational parameter is in units of fm^{-2} .

Meson	J/ψ	η_c	Υ	η_b	B_c	B_c^*
Theoretical masses	3092.2	2998.5	9468.9	9389.0	6287.9	6350.5
Variational parameters	12.5	15.0	49.7	57.4	22.9	20.2
Experiment masses	3096.9	2983.9	9460.3	9399.0	6274.9	
Error	-4.7	14.6	8.6	10.0	13.0	

Moreover, we have systemically construct the total wave function satisfied with Pauli Principle in the previous section. The corresponding total wave function could be expanded as follows:

$$|\Psi_\alpha\rangle = \sum_{ij} C_{ij}^\alpha |F\rangle |R^s\rangle |[\phi_i \chi_j]\rangle. \quad (10)$$

To investigate the mass of the fully heavy tetraquarks with the variational method, we calculate the Schrödinger equation $H|\Psi_\alpha\rangle = E_\alpha|\Psi_\alpha\rangle$, diagonalize the corresponding matrix, and then determine the ground state masses for the fully heavy tetraquarks. According to corresponding variational parameters, we further give the internal mass contributions, including quark masses part, kinetic energy part, confinement potential part, and hyperfine potential part. As a comparison, we also show the lowest meson-meson thresholds for the tetraquarks with different quantum numbers and their internal contributions. Thus, we define the binding energy:

$$B_T = M_{tetraquark} - M_{meson1} - M_{meson2}, \quad (11)$$

where $M_{tetraquark}$, M_{meson1} , and M_{meson2} are masses of tetraquark and the two mesons at lowest threshold allowed in the rearrangement decay of the tetraquark, respectively. In order to discuss conveniently in next subsection, we also define the V^C : the sum of Coulomb potential and linear potential.

Lastly, it is also useful to investigate the spatial size of the tetraquarks which strongly relates to the magnitude of the various kinetic energies and the potential energies between quarks. Understanding the relative lengths between quarks in tetraquarks and their lowest thresholds

is also important, and the relative distance between the heavier quarks is, in general, shorter than that between the lighter quarks [47]. This tendency is also maintained in each tetraquark state according to corresponding Tables.

In the following subsections, we concretely discuss all possible configurations for fully heavy tetraquarks.

A. $cc\bar{c}\bar{c}$ and $bb\bar{b}\bar{b}$ states

Firstly, we investigate the $cc\bar{c}\bar{c}$ and $bb\bar{b}\bar{b}$ systems. There are two $J^{PC} = 0^{++}$ states, a $J^{PC} = 1^{+-}$ state, and a $J^{PC} = 2^{++}$ state according to Table IV. We show the eigenvalue of the hyperfine factor for the ground states and their possible decay channels in Table VI. Moreover, we also show the masses of ground states, variational parameters, the internal mass contributions, the relative lengths between quarks, and their lowest meson-meson thresholds in Table VII, respectively.

Here, we take the ground $J^{PC} = 0^{++}$ $bb\bar{b}\bar{b}$ state as an example, and others have similar discussions according to Tables VI and VII. According to Table VI, the eigenvalues for ground states are not equal to expectation values for two meson states. Moreover, we also find the ground $J^{PC} = 0^{++}$ $bb\bar{b}\bar{b}$ state has a smaller eigenvalue and thus less attractive than the $\eta_b\eta_b$ decay channel, but is still more attractive than $\Upsilon\Upsilon$ decay channel. Nevertheless, the reason why this state has energy obviously larger than $\eta_b\eta_b$ and $\Upsilon\Upsilon$ decay channels is that the contribution from the confinement potential is obviously larger than those of $\eta_b\eta_b$ and $\Upsilon\Upsilon$ decay channels. Hence, it should be a compact state, but is not a stable state, which can decay into rearrangement decay channels.

We now analyze the numerical results obtained from the variational method. As for the ground $J^{PC} = 0^{++}$ $bb\bar{b}\bar{b}$ state, its mass is 19240.0 MeV, and corresponding binding energy B_T is +461.9 MeV. The total wave function is given as:

$$|\Psi_{tot}\rangle = 0.936|F\rangle|R^s\rangle|\phi_2\chi_6\rangle - 0.352|F\rangle|R^s\rangle|\phi_1\chi_5\rangle. \quad (12)$$

Its variational parameters are given as $C_{11} = 7.7 \text{ fm}^{-2}$, $C_{22} = 7.7 \text{ fm}^{-2}$, and $C_{33} = 11.4 \text{ fm}^{-2}$, which shows roughly the inverse ratios of size for diquark, antidiquark, and between the center of diquark and antidiquark, respectively. We naturally find that the C_{11} is equal to C_{22} , hence the distance of $(b - b)$ would be equal to that of $(\bar{b} - \bar{b})$, and the reason is that $bb\bar{b}\bar{b}$ system is a neutral system.

1. The relative distances and symmetry

Here, we concentrate on the the relative distances between the (anti)quarks in tetraquarks. Looking into the

relative distances in Table VII, we find that the relative distances of (1,2) and (3,4) pairs are same, and other relative distances are same in all the $cc\bar{c}\bar{c}$ and $bb\bar{b}\bar{b}$ states. This is because of the permutation symmetry for the ground state wave function in each tetraquarks [51]. For the $c_1c_2\bar{c}_3\bar{c}_4$ and $b_1b_2\bar{b}_3\bar{b}_4$ states, they need to satisfy the Pauli principle for identical particles are as follows:

$$A_{12}|\Psi_{tot}\rangle = A_{34}|\Psi_{tot}\rangle = -|\Psi_{tot}\rangle, \quad (13)$$

where the operation A_{ij} means exchanging the coordinate of Q_i (\bar{Q}_i) and Q_j (\bar{Q}_j).

Meanwhile, they are pure neutral particles with definite C-parity, so the permutation symmetries for total wave functions as follows:

$$A_{12-34}|\Psi_{tot}\rangle = \pm|\Psi_{tot}\rangle, \quad (14)$$

where A_{12-34} means exchanging the coordinate of diquark and antidiquark.

Based on these, the relationship of relative distances for all the $c_1c_2\bar{c}_3\bar{c}_4$ and $b_1b_2\bar{b}_3\bar{b}_4$ states can be obtained as follows:

$$\begin{aligned} & \langle\Psi_{tot}|\mathbf{r}_1 - \mathbf{r}_3|\Psi_{tot}\rangle \\ &= \langle\Psi_{tot}|A_{12}^{-1}A_{12}|\mathbf{r}_1 - \mathbf{r}_3|A_{12}^{-1}A_{12}|\Psi_{tot}\rangle = \langle\Psi_{tot}|\mathbf{r}_2 - \mathbf{r}_3|\Psi_{tot}\rangle \\ &= \langle\Psi_{tot}|A_{34}^{-1}A_{34}|\mathbf{r}_2 - \mathbf{r}_3|A_{34}^{-1}A_{34}|\Psi_{tot}\rangle = \langle\Psi_{tot}|\mathbf{r}_2 - \mathbf{r}_4|\Psi_{tot}\rangle \\ &= \langle\Psi_{tot}|A_{12}^{-1}A_{12}|\mathbf{r}_2 - \mathbf{r}_4|A_{12}^{-1}A_{12}|\Psi_{tot}\rangle = \langle\Psi_{tot}|\mathbf{r}_1 - \mathbf{r}_4|\Psi_{tot}\rangle, \end{aligned} \quad (15)$$

and

$$\begin{aligned} & \langle\Psi_{tot}|\mathbf{r}_1 - \mathbf{r}_2|\Psi_{tot}\rangle \\ &= \langle\Psi_{tot}|A_{12-34}^{-1}A_{12-34}|\mathbf{r}_1 - \mathbf{r}_2|A_{12-34}^{-1}A_{12-34}|\Psi_{tot}\rangle \\ &= \langle\Psi_{tot}|\mathbf{r}_3 - \mathbf{r}_4|\Psi_{tot}\rangle. \end{aligned} \quad (16)$$

Obviously, our theoretical derivations are in perfect agreement with the calculated results in Table VII.

Further, we can also prove three Jacobi coordinates, $\mathbf{R}_{1,2} = \mathbf{r}_1 - \mathbf{r}_2$, $\mathbf{R}_{3,4} = \mathbf{r}_3 - \mathbf{r}_4$, and $\mathbf{R}' = 1/2(\mathbf{r}_1 + \mathbf{r}_2 - \mathbf{r}_3 - \mathbf{r}_4)$, are orthogonal to each other for all the $cc\bar{c}\bar{c}$ and $bb\bar{b}\bar{b}$ states:

$$\begin{aligned} & \langle\Psi_{tot}|\mathbf{R}_{1,2} \cdot \mathbf{R}_{3,4}|\Psi_{tot}\rangle \\ &= \langle\Psi_{tot}|(34)^{-1}(34)|\mathbf{R}_{1,2} \cdot \mathbf{R}_{3,4}|(34)^{-1}(34)|\Psi_{tot}\rangle \\ &= -\langle\Psi_{tot}|\mathbf{R}_{1,2} \cdot \mathbf{R}_{3,4}|\Psi_{tot}\rangle = 0, \end{aligned} \quad (17)$$

$$\begin{aligned} & \langle\Psi_{tot}|\mathbf{R}_{1,2} \cdot \mathbf{R}'|\Psi_{tot}\rangle \\ &= \langle\Psi_{tot}|(12)^{-1}(12)|\mathbf{R}_{1,2} \cdot \mathbf{R}'|(12)^{-1}(12)|\Psi_{tot}\rangle \\ &= -\langle\Psi_{tot}|\mathbf{R}_{1,2} \cdot \mathbf{R}'|\Psi_{tot}\rangle = 0, \end{aligned} \quad (18)$$

and

$$\begin{aligned} & \langle\Psi_{tot}|\mathbf{R}_{3,4} \cdot \mathbf{R}'|\Psi_{tot}\rangle \\ &= \langle\Psi_{tot}|\mathbf{R}_{3,4} \cdot \mathbf{R}'|\Psi_{tot}\rangle \\ &= \langle\Psi_{tot}|\mathbf{R}_{3,4} \cdot \mathbf{R}'|\Psi_{tot}\rangle = 0, \end{aligned} \quad (19)$$

According to the relative distances in Table VII and the relationship of Eqs. (13-18), we can well describe the

TABLE VI. The expectation value of the hyperfine factor for the $cc\bar{c}\bar{c}$ and $bb\bar{b}\bar{b}$ systems and their possible decay channels. (unit: $(\text{GeV})^{-2}$)

Systems	$cc\bar{c}\bar{c}$			$bb\bar{b}\bar{b}$		
	0^{++}	1^{+-}	2^{++}	0^{++}	1^{+-}	2^{++}
J^{PC}						
$\langle \sum_{i<j}^4 -\frac{1}{m_i m_j} \lambda_i^c \cdot \lambda_j^c \sigma_i \cdot \sigma_j \rangle$	$\left(\frac{16}{3m_c^2} - \frac{32}{3m_c m_{\bar{c}}} \frac{8\sqrt{6}}{m_c m_{\bar{c}}} \right)$	$\left(\frac{16}{3m_c^2} - \frac{16}{3m_c m_{\bar{c}}} \right)$	$\left(\frac{16}{3m_c^2} + \frac{16}{3m_c m_{\bar{c}}} \right)$	$\left(\frac{16}{3m_b^2} - \frac{32}{3m_b m_{\bar{b}}} \frac{8\sqrt{6}}{m_b m_{\bar{b}}} \right)$	$\left(\frac{16}{3m_b^2} - \frac{16}{3m_b m_{\bar{b}}} \right)$	$\left(\frac{16}{3m_b^2} + \frac{16}{3m_b m_{\bar{b}}} \right)$
Lowest Eigenvalue	-5.26	0	2.90	-0.68	0	0.37
Decay channel	$J/\psi J/\psi$	$J/\psi \eta_c$	$\eta_c \eta_c$	$\Upsilon \Upsilon$	$\Upsilon \eta_c$	$\eta_b \eta_b$
$\langle -\frac{1}{m_i m_j} \lambda_i^c \cdot \lambda_j^c \sigma_i \cdot \sigma_j \rangle$	$\frac{16}{3m_c m_{\bar{c}}} + \frac{16}{3m_c m_{\bar{c}}}$	$\frac{16}{3m_c m_{\bar{c}}} - \frac{16}{m_c m_{\bar{c}}}$	$-\frac{16}{m_c m_{\bar{c}}} - \frac{16}{m_c m_{\bar{c}}}$	$\frac{16}{3m_b m_{\bar{b}}} + \frac{16}{3m_b m_{\bar{b}}}$	$\frac{16}{3m_b m_{\bar{b}}} - \frac{16}{m_b m_{\bar{b}}}$	$-\frac{16}{m_b m_{\bar{b}}} - \frac{16}{m_b m_{\bar{b}}}$
Quantum number	$0^{++}, 2^{++}$	1^{+-}	0^{++}	$0^{++}, 2^{++}$	1^{+-}	0^{++}
Value	2.90	-2.90	-8.70	0.37	-0.37	-1.12

TABLE VII. The masses, variational parameters, the contribution, and the relative lengths between quarks for $cc\bar{c}\bar{c}$, $bb\bar{b}\bar{b}$ systems, corresponding lowest meson-meson thresholds, and their differences (D_0 , D_1 , or D_2). The number is given as $i=1,2$ for the quarks, and $3,4$ for the antiquarks. The masses, B_T , and contributions are in MeV unit. The relative lengths (variational parameters) are fm (fm^{-2}) unit.

Systems		$cc\bar{c}\bar{c}$								$bb\bar{b}\bar{b}$									
J^{PC}	(i,j)	0^{++}	$\eta_c \eta_c$	D_0	1^{+-}	$J/\psi \eta_c$	D_1	2^{++}	$J/\psi J/\psi$	D_2	0^{++}	$\eta_b \eta_b$	D_0	1^{+-}	$\Upsilon \eta_b$	D_1	2^{++}	$\Upsilon \Upsilon$	D_2
Mass/ B_T		6384.4	5997.0	387.4	6451.5	6090.7	360.8	6482.7	6184.5	298.2	19240.0	18778.1	461.9	19303.9	18857.9	446.0	19327.9	18937.8	390.1
Variational Parameters (fm^{-2})	C_{11}	7.7	15.0		9.1	15.0		8.9	12.5		24.6	57.4		30.7	57.4		30.0	49.7	
	C_{22}	7.7	15.0		9.1	12.5		8.9	12.5		24.6	57.4		30.7	49.7		30.0	49.7	
	C_{33}	11.4			7.3			6.9				39.5		24.0			23.0		
Quark Mass		7672.0	7672.0	0.0	7672.0	7672.0	0.0	7672.0	7672.0	0.0	21372.0	21372.0	0.0	21372.0	21372.0	0.0	21372.0	21372.0	0.0
Confinement Potential		-2083.8	-2440.4	356.6	-1998.8	-2367.4	368.6	-1973.6	-2294.4	320.8	-3101.0	-3724.2	623.2	-3003.4	-3641.9	638.5	-2977.3	-3559.5	582.2
Kinetic Energy		814.0	915.1	-101.1	767.2	839.0	-71.8	752.0	762.9	-10.9	970.4	1255.9	-285.5	934.0	1171.6	-237.6	908.1	1087.3	-179.2
CS Interaction		22.7	-150.0	172.7	1.5	-52.9	54.4	32.3	43.9	-11.6	17.0	-125.5	142.5	1.3	-43.8	45.1	25.1	38.0	-12.9
V^C	(1,2)	-6.8			-19.4			-14.6			111.8			-274.5			-269.1		
	(1,3)	-26.1	-237.2(η_c)		1.5	-237.2(η_c)		5.4	-164.2(J/ψ)		-339.7	-879.1(η_b)		-122.1	-879.1(η_b)		-118.3	-796.7(Υ)	
	(2,3)	-26.1			1.5			5.4			-339.7			-122.1			-118.3		
	(1,4)	-26.1			1.5			5.4			-339.7			-122.1			-118.3		
	(2,4)	-26.1	-237.2(η_c)		1.5	-164.2(J/ψ)		5.4	-164.2(J/ψ)		-339.7	-879.1(η_b)		-122.1	-796.7(Υ)		-118.3	-796.7(Υ)	
	(3,4)	-6.8			-19.4			-14.6			111.8			-274.5			-269.1		
	Total		-117.8	-474.4	356.6	-32.8	-401.4	368.6	-7.6	-328.4	320.8	-1135.0	-1758.2	623.2	-1037.4	-1675.9	632.5	-1011.3	-1593.5
Total Contribution		718.9	291.0	427.9	745.5	384.7	360.8	776.7	478.5	298.2	-147.6	-627.9	480.3	-102.1	-548.1	446.0	-78.1	-468.2	390.1
Relative Lengths (fm)	(1,2)	0.406			0.373			0.377			0.227			0.203			0.205		
	(1,3)	0.371	0.290(η_c)		0.395	0.290(η_c)		0.403	0.318(J/ψ)		0.204	0.148(η_b)		0.217	0.148(η_b)		0.220	0.160(Υ)	
	(2,3)	0.371			0.395			0.403			0.204			0.217			0.220		
	(1,4)	0.371			0.395			0.403			0.204			0.217			0.220		
	(2,4)	0.371	0.290(η_c)		0.395	0.318(J/ψ)		0.403	0.318(J/ψ)		0.204	0.148(η_b)		0.217	0.160(Υ)		0.220	0.160(Υ)	
	(3,4)	0.406			0.373			0.377			0.227			0.203			0.205		
	(1,2)-(3,4)	0.235			0.294			0.302			0.126			0.162			0.165		
Radius(fm)		0.235			0.237			0.241			0.130			0.130			0.132		

relative positions of the four valence quarks for all the $cc\bar{c}\bar{c}$ and $bb\bar{b}\bar{b}$ states. Meanwhile, using the relative distances between (anti)quarks and orthogonal relationship, one can also determine the relative distance of (12)–(34), and it is consistent with our results in Table VII. Further,

we can give the relative position of R_c and the spherical radius of the tetraquarks. Here, we define that the R_c is the geometric center of the four quarks (the center of the sphere). Based on these results, we show the spatial distribution of four valence quarks for the ground

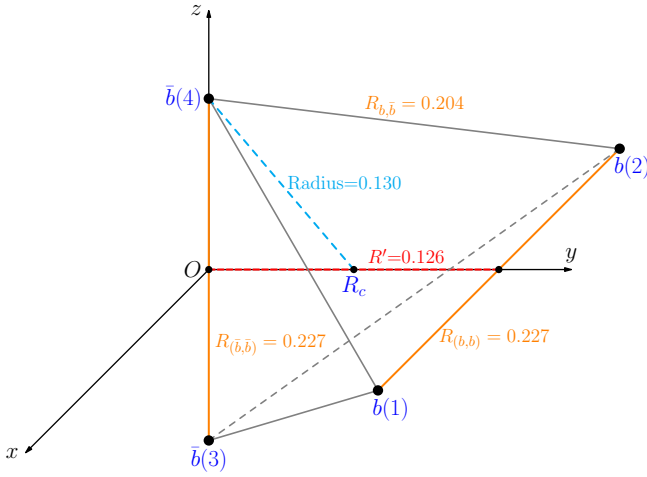


FIG. 1. Relative positions for four valence quarks and R_c in the $J^{PC} = 0^{++}$ ground $bb\bar{b}\bar{b}$ state. Meanwhile, we label the relative distances of $R_{b,b}$, $R_{b,\bar{b}}$, $R_{\bar{b},\bar{b}}$, R' , and the radius (units: fm).

$J^{PC} = 0^{++}$ $bb\bar{b}\bar{b}$ state in Fig. 1.

2. The internal contribution

Here, let us now turn our discussion to the internal mass contribution for the ground $J^{PC} = 0^{++}$ $bb\bar{b}\bar{b}$ state.

Firstly, for the kinetic energy, this $bb\bar{b}\bar{b}$ state has 814.0 MeV, which can be understood as the sum of three internal kinetic energies: kinetic energies of two pairs of the $b - \bar{b}$, and the $(b\bar{b}) - (b\bar{b})$ pair. Accordingly, the sum of the internal kinetic energies of $\eta_b\eta_{\bar{b}}$ state only come from the two pairs of the $b - \bar{b}$. Therefore, this $bb\bar{b}\bar{b}$ state has an additional kinetic energy needed to bring the $\eta_b\eta_{\bar{b}}$ into a compact configuration. The actual kinetic energies of two pairs of the $b - \bar{b}$ in the the ground $J^{PC} = 0^{++}$ $bb\bar{b}\bar{b}$ state are smaller than those inside the $\eta_b\eta_{\bar{b}}$ state. This is so because as can be seen in Table VII, the distance of $b - \bar{b}$ in the tetraquark state is larger than in the meson: the distance of $b - \bar{b}$ is 0.204 fm in this $bb\bar{b}\bar{b}$ state while it is 0.148 fm in η_b . Meanwhile, we find even if considering the additional kinetic energy between the $(b\bar{b}) - (b\bar{b})$ pair, the total kinetic energies in this $bb\bar{b}\bar{b}$ state is still smaller than that of the $\eta_b\eta_{\bar{b}}$ state. However, this does not cause the ground $J^{PC} = 0^{++}$ $bb\bar{b}\bar{b}$ state to a stable state due to confinement potential part.

As for the confinement potential part, the contributions from V^C for the ground $J^{PC} = 0^{++}$ $bb\bar{b}\bar{b}$ state in Table VII are all attractive. Thus, this state has a large positive binding energy. However, it still above the meson-meson threshold because the $V^C(b\bar{b})$ in η_b is much attractive. As for other internal contributions, the quark contents of this state are the same as its corresponding rearrangement decay threshold. Moreover, the mass contribution from the hyperfine potential term is negligible relative to the contributions from other terms.

B. $cc\bar{b}\bar{b}$ state

Here, we concentrate on the $cc\bar{b}\bar{b}$ system. Similar to the $cc\bar{c}\bar{c}$ and $bb\bar{b}\bar{b}$ systems, the $cc\bar{b}\bar{b}$ system is also satisfied with fully antisymmetric for diquark and antiquark. There are two $J^P = 0^+$ states, a $J^P = 1^+$ state, and a $J^P = 2^+$ state in $cc\bar{b}\bar{b}$ system. We show the eigenvalue of the hyperfine factor for the ground states and their possible decay channels in Table VIII. Moreover, we also show the masses of ground states, corresponding variational parameters, different internal mass contributions, the relative lengths between quarks, and their lowest meson-meson threshold in Table IX, respectively.

TABLE VIII. The expectation value of the hyperfine factor for the $cc\bar{b}\bar{b}$ system and their possible decay channels. (unit: $(\text{GeV})^{-2}$)

System	$cc\bar{b}\bar{b}$		
J^P	0^+		
$\langle \sum_{i<j}^4 \frac{-1}{m_i m_j} \lambda_i^c \cdot \lambda_j^c \sigma_i \cdot \sigma_j \rangle$	$\left(\frac{8}{3m_c^2} + \frac{8}{3m_b^2} - \frac{32}{3m_c m_b} \frac{8\sqrt{6}}{m_c m_b} \right)$		
Lowest Eigenvalue	-1.845		
J^P	1^+	2^+	
$\langle \sum_{i<j}^4 \frac{-1}{m_i m_j} \lambda_i^c \cdot \lambda_j^c \sigma_i \cdot \sigma_j \rangle$	$\left(\frac{8}{3m_c^2} + \frac{8}{3m_b^2} - \frac{16}{3m_c m_b} \right)$	$\left(\frac{8}{3m_c^2} + \frac{8}{3m_b^2} + \frac{16}{3m_c m_b} \right)$	
Lowest Eigenvalue	0.298	1.339	
Decay channel	$B_c^* B_c^*$	$B_c^* B_c$	$B_c B_c$
$\langle \frac{-1}{m_i m_j} \lambda_i^c \cdot \lambda_j^c \sigma_i \cdot \sigma_j \rangle$	$\frac{16}{3m_c m_b} + \frac{16}{3m_c m_b}$	$\frac{16}{3m_c m_b} - \frac{16}{m_c m_b}$	$\frac{-16}{m_c m_b} - \frac{16}{m_c m_b}$
Quantum number	$0^+, 2^+$	1^+	0^+
Value	1.041	-1.041	-3.123

Firstly, to compare the hyperfine factors of the $cc\bar{b}\bar{b}$ tetraquarks with the corresponding sum of two mesons in the possible decay channels, we need to obtain and diagonalize $\langle \sum_{i<j}^4 -\frac{1}{m_i m_j} \lambda_i^c \cdot \lambda_j^c \sigma_i \cdot \sigma_j \rangle$ to get the the corresponding eigenvalues. The corresponding results are shown in Table VIII. The $B_c B_c$ system is more attractive than any $cc\bar{b}\bar{b}$ state. The ground $J^P = 0^+$ $cc\bar{b}\bar{b}$ state is also less attractive than the $B_c B_c$ decay channel but still more attractive than the $B_c^* B_c^*$ decay channel. Thus, it can decay into rearrangement decay channels and is not a stable state.

Next, we take the ground $J^P = 0^+$ $cc\bar{b}\bar{b}$ state as an example to discuss its properties with the variational method. Similar situation also happens in other two quantum numbers according to Tables VIII and IX. The mass of the lowest $J^P = 0^+$ $cc\bar{b}\bar{b}$ state is 12920.0 MeV, and corresponding binding energy B_T is +344.2 MeV according to Table VIII. Thus, the state is obviously higher than the corresponding rearrangement meson-meson thresholds. The wave function is given as:

$$|\Psi_{tot}\rangle = 0.966|F\rangle|R^s\rangle|[\phi_1\chi_5]\rangle - 0.259|F\rangle|R^s\rangle|[\phi_2\chi_6]\rangle. \quad (20)$$

Here, we notice that the mass contribution of ground state mainly come from the $|(Q_1 Q_2)_1^3 (Q_3 \bar{Q}_4)_1^3|_0$ com-

TABLE IX. The masses, variational parameters, the contribution, and the relative lengths between quarks for $cc\bar{b}\bar{b}$ system, corresponding lowest meson-meson thresholds, and their differences (D_0 , D_1 , or D_2). The number is given as $i=1,2$ for the quarks, and $3,4$ for the antiquarks. The masses, B_T , and contributions are in MeV unit. The relative lengths (variational parameters) are fm (fm^{-2}) unit.

System		$cc\bar{b}\bar{b}$									
J^{PC}	(i,j)	0^+	$B_c B_c$	D_0	1^+	$B_c^* B_c$	D_1	2^+	$B_c^* B_c^*$	D_2	
Mass/ B_T		12920.0	12575.8	344.2	12939.9	12638.4	301.5	12960.9	12700.9	260.0	
Variational Parameters (fm^{-2})	C_{11}	23.9	22.9		24.8	20.2		24.5	20.2		
	C_{22}	10.5	22.9		10.3	22.9		10.1	20.2		
	C_{33}	12.3			11.1			10.7			
Quark Mass		14522.0	14522.0	0.0	14522.0	14522.0	0.0	14522.0	14522.0	0.0	
Confinement Potential		-2420.1	-2795.5	375.4	-2400.7	-2741.1	340.4	-2382.1	-2686.8	304.7	
Kinetic Energy		835.9	947.3	-111.4	814.0	891.5	-77.5	795.6	835.7	-40.1	
CS Interaction		-7.0	-98.0	91.0	4.6	-34.0	38.6	25.3	30.0	-4.7	
V^C	(1,2)	-271.1			-225.5			-222.4			
	(1,3)	-47.5	-414.8(B_c)		-41.6	-360.4(B_c^*)		-38.7	-360.4(B_c^*)		
	(2,3)	-47.5			-41.6			-38.7			
	(1,4)	-47.5			-41.6			-38.7			
	(2,4)	-47.5	-414.8(B_c)		-41.6	-414.8(B_c)		-38.7	-360.4(B_c^*)		
	(3,4)	-46.9			-43.0			-38.9			
	Total	-454.0	-829.5	375.3	-434.7	-775.1	340.4	-416.0	-720.8	304.8	
Total Contribution		374.9	19.8	355.1	383.9	82.4	301.5	404.9	144.9	260.0	
Relative Lengths (fm)	(1,2)	0.230			0.226			0.227			
	(1,3)	0.308	0.235(B_c)		0.317	0.250(B_c^*)		0.322	0.250(B_c^*)		
	(2,3)	0.308			0.317			0.322			
	(1,4)	0.308			0.317			0.322			
	(2,4)	0.308	0.235(B_c)		0.317	0.235(B_c)		0.322	0.250(B_c^*)		
	(3,4)	0.348			0.351			0.355			
	(1,2)-(3,4)	0.226			0.238			0.243			

ponent, and the $|(Q_1 Q_2)_0^6 (\bar{Q}_3 \bar{Q}_4)_0^6\rangle$ component is negligible. Its variational parameters are given as $C_{11} = 23.9\text{fm}^{-2}$, $C_{22} = 10.5\text{fm}^{-2}$, and $C_{33} = 12.3\text{fm}^{-2}$.

Let us now turn our discussion to the internal contribution for the ground $cc\bar{b}\bar{b}$ state. For the kinetic energy part, the $J^P = 0^+$ $cc\bar{b}\bar{b}$ state obtains 835.9 MeV, which is smaller than that of the meson-meson threshold $B_c B_c$. The potential part of this state is far smaller than that of the lowest meson-meson threshold. Further, we notice that all the V^C for this state are attractive. However, relative to the V^C of $B_c B_c$, these attractive values seem to trivial. This is because the length between $c - \bar{b}$ in tetraquarks is longer than that in B_c according to Table IX. In summary, we tend to think these $cc\bar{b}\bar{b}$ states are unstable compact states.

C. $cc\bar{b}\bar{b}$ and $bb\bar{c}\bar{c}$ states

Here, we discuss the $cc\bar{b}\bar{b}$ and $bb\bar{c}\bar{c}$ systems. For these two system, they only need to satisfy the antisymmetry for the diquark. Thus, comparing to above three systems, the $cc\bar{b}\bar{b}$ and $bb\bar{c}\bar{c}$ systems have more allowed states. There are two $J^P = 0^+$ states, three $J^P = 1^+$ states, one $J^P = 2^+$ state in the $cc\bar{b}\bar{b}$ and $bb\bar{c}\bar{c}$ systems. We show the eigenvalue of the hyperfine factor for the ground states and their possible decay channels in Table VIII. Moreover, we calculate the masses of ground states, corresponding variational parameters, different internal contributions, the relative lengths between quarks, and their lowest meson-meson threshold in Table XI, respectively.

Firstly, we compare the expectation values of the hyperfine factor of the tetraquarks with the corresponding sum of two mesons in Table VIII. For the $bb\bar{c}\bar{c}$ system, we notice that the $\eta_c B_c$ decay channel is the most attractive channel. Moreover, the $J^P = 1^+$ ground state is more at-

TABLE X. The expectation value of the hyperfine factor for the $cc\bar{c}\bar{b}$, $bb\bar{b}\bar{c}$ systems and their possible decay channels. (unit: $(\text{GeV})^{-2}$)

Systems	$cc\bar{c}\bar{b}$				$bb\bar{b}\bar{c}$			
J^P	0^+				0^+			
$\langle \sum_{i<j}^4 \frac{-1}{m_i m_j} \lambda_i^c \cdot \lambda_j^c \sigma_i \cdot \sigma_j \rangle$	$\left(\frac{8}{3m_c^2} + \frac{8}{3m_\varepsilon m_b} - \frac{16}{3m_c m_b} - \frac{16}{3m_c m_\varepsilon} \frac{4\sqrt{6}}{m_c m_b} + \frac{4\sqrt{6}}{m_c m_\varepsilon} \right)$				$\left(\frac{8}{3m_b^2} + \frac{8}{3m_\varepsilon m_b} - \frac{16}{3m_b m_\varepsilon} - \frac{16}{3m_b m_b} \frac{4\sqrt{6}}{m_b m_\varepsilon} + \frac{4\sqrt{6}}{m_b m_b} \right)$			
Low Eigenvalue	-3.58				-1.28			
J^P	1^+				1^+			
$\langle \sum_{i<j}^4 \frac{-1}{m_i m_j} \lambda_i^c \cdot \lambda_j^c \sigma_i \cdot \sigma_j \rangle$	$\left(\frac{8}{3m_c^2} + \frac{8}{3m_\varepsilon m_b} - \frac{8}{3m_c m_b} - \frac{8}{3m_c m_\varepsilon} \frac{8\sqrt{2}}{3m_c m_\varepsilon} - \frac{8\sqrt{2}}{3m_c m_b} \frac{8}{m_c m_\varepsilon} - \frac{8}{m_c m_b} \frac{8}{m_c m_\varepsilon} - \frac{8}{m_c m_b} \frac{8}{m_c m_\varepsilon} \right)$				$\left(\frac{8}{3m_b^2} + \frac{8}{3m_\varepsilon m_b} - \frac{8}{3m_b m_\varepsilon} - \frac{8}{3m_b m_b} \frac{8\sqrt{2}}{3m_b m_b} - \frac{8\sqrt{2}}{3m_b m_b} \frac{8}{m_b m_\varepsilon} - \frac{8}{m_b m_b} \frac{8}{m_b m_\varepsilon} - \frac{8}{m_b m_b} \frac{8}{m_b m_\varepsilon} \right)$			
Low Eigenvalue	-2.49				-1.34			
J^P	2^+				2^+			
$\langle \sum_{i<j}^4 \frac{-1}{m_i m_j} \lambda_i^c \cdot \lambda_j^c \sigma_i \cdot \sigma_j \rangle$	$\left(\frac{8}{3m_c^2} + \frac{8}{3m_\varepsilon m_b} + \frac{8}{3m_c m_b} + \frac{8}{3m_c m_\varepsilon} \right)$				$\left(\frac{8}{3m_b^2} + \frac{8}{3m_\varepsilon m_b} + \frac{8}{3m_b m_\varepsilon} + \frac{8}{3m_b m_b} \right)$			
Lowest Eigenvalue	1.97				0.71			
Decay channel	$J/\psi B_c^*$	$J/\psi B_c$	$\eta_c B_c^*$	$\eta_c B_c$	ΥB_c^*	ΥB_c	$\eta_b B_c^*$	$\eta_b B_c$
$\langle -\frac{1}{m_i} \lambda_i^c \cdot \lambda_j^c \sigma_i \cdot \sigma_j \rangle$	$\frac{16}{3m_c m_\varepsilon} + \frac{16}{3m_c m_b}$	$\frac{16}{3m_c m_\varepsilon} - \frac{16}{m_c m_b}$	$-\frac{16}{m_c m_\varepsilon} + \frac{16}{3m_c m_b}$	$-\frac{16}{m_c m_\varepsilon} - \frac{16}{m_c m_b}$	$\frac{16}{3m_b m_b} + \frac{16}{3m_c m_b}$	$\frac{16}{3m_b m_b} - \frac{16}{m_c m_b}$	$-\frac{16}{m_b m_b} + \frac{16}{3m_b m_b}$	$-\frac{16}{m_b m_b} - \frac{16}{m_c m_b}$
Quantum number	$0^+, 1^+, 2^+$	1^+	1^+	0^+	$0^+, 1^+, 2^+$	1^+	1^+	0^+
Value	1.97	-0.11	-3.83	-5.91	0.71	-1.37	-0.04	-2.12

TABLE XI. The masses, variational parameters, the internal contribution, and the relative lengths between quarks for $bb\bar{b}\bar{c}$ and $cc\bar{c}\bar{b}$ systems, corresponding lowest meson-meson thresholds, and their differences (D_0 , D_1 , or D_2). The number is given as $i=1,2$ for the quarks, and $3,4$ for the antiquarks. The masses, B_T , and contributions are in MeV unit. The relative lengths (variational parameters) are fm (fm^{-2}) unit.

Systems		$bb\bar{b}\bar{c}$								$cc\bar{c}\bar{b}$									
J^{PC}	(i,j)	0^+	$B_c \eta_b$	D_0	1^+	$B_c^* \eta_b$	D_1	2^+	$B_c^* \Upsilon$	D_2	0^+	$B_c \eta_c$	D_0	1^+	$B_c^* \eta_c$	D_1	2^+	$B_c^* J/\psi$	D_2
Mass/ B_T		16043.9	15676.9	367.0	16043.2	15739.5	303.7	16149.2	15819.4	329.8	9620.5	9286.4	334.1	9624.6	9349.0	275.6	9730.5	9442.7	287.8
Variational Parameters (fm ⁻²)	C_{11}	12.5	22.9		12.4	20.2		14.4	20.2		11.4	22.9		11.1	20.2		13.7	20.2	
	C_{22}	21.7	58.8		21.0	57.4		28.6	49.7		7.2	15.0		6.9	15.0		8.9	12.5	
	C_{33}	28.7			28.9			16.9			15.2			15.3			9.1		
Quark Mass		17947.0	17947.0	0.0	17947.0	17947.0	0.0	17947.0	17947.0	0.0	11097.0	11097.0	0.0	11097.0	11097.0	0.0	11097.0	11097.0	0.0
Confinement Potential		-2786.7	-3259.9	473.2	-2779.8	-3205.5	425.7	-2659.7	-3123.1	463.4	-2280.0	-2618.0	338.0	-2266.2	-2563.6	297.4	-2158.4	-2490.6	332.2
Kinetic Energy		883.3	1101.6	-218.3	876.1	1045.8	-169.7	838.2	961.5	-123.3	810.3	931.2	-120.9	795.2	875.4	-80.2	763.9	799.3	-35.4
CS Interaction		15.5	-111.8	127.3	4.8	-47.8	52.6	23.8	34.0	-10.2	18.2	-123.8	142.0	8.0	-59.9	67.9	28.0	36.9	-8.9
V^C	(1,2)	40.8			39.7			-110.1			32.0			29.0			-99.6		
	(1,3)	-251.3			-248.2			-85.5			-91.9			-87.0			-21.9		
	(2,3)	-228.3	-879.1(η_b)		-225.8	-879.1(η_b)		-77.6	-164.2(Υ)		-74.8	-879.1(η_c)		-68.9	-879.1(η_c)		-17.3	-164.2(J/ψ)	
	(1,4)	-251.3	-414.8(B_c)		-248.2	-360.4(B_c^*)		-85.5	-360.4(B_c^*)		-91.9	-414.8(B_c)		-87.0	-360.4(B_c^*)		-21.9	-360.4(B_c^*)	
	(2,4)	-228.3			-225.8			-77.6			-74.8			-68.9			-17.3		
	(3,4)	97.7			94.5			-257.5			-12.7			-17.4			-14.3		
	Total		-820.7	-1293.9	473.2	-813.8	-1239.5	425.7	-693.7	-1157.1	463.4	-314.0	-652.0	338.0	-300.2	-597.6	297.4	-192.4	-524.6
Total Contribution		78.1	-304.1	382.2	67.1	-241.5	308.6	168.2	-161.6	329.8	514.4	155.4	359.0	503.0	218.0	285.0	599.5	311.7	287.8
Relative Lengths (fm)	(1,2)	0.318	0.235(B_c)		0.320	0.250(B_c^*)		0.296	0.250(B_c^*)		0.333	0.235(B_c)		0.338	0.250(B_c^*)		0.304	0.250(B_c^*)	
	(1,3)	0.239			0.240			0.256			0.325			0.328			0.350		
	(2,3)	0.249			0.250			0.266			0.336			0.340			0.359		
	(1,4)	0.239			0.240			0.256			0.325			0.328			0.350		
	(2,4)	0.249			0.250			0.266			0.336			0.340			0.359		
	(3,4)	0.242	0.148(η_b)		0.245	0.148(η_b)		0.210	0.160(Υ)		0.418	0.290(η_c)		0.429	0.290(η_c)		0.378	0.318(J/ψ)	
	(1,2)-(3,4)	0.148			0.148			0.194			0.204			0.203			0.264		

tractive than others, and meanwhile, it only slightly less attractive than the ΥB_c decay channel. Therefore, we can expect to have a compact stable state for $J^P = 1^+ bb\bar{b}\bar{c}$ configuration when considering the hyperfine potential only.

Based on these, we now analyse the numerical results of the $J^P = 1^+$ ground $bb\bar{b}\bar{c}$ state obtained from the variational method according to Table XI. Other states would have similar discussions from Tables VIII and XI. The mass of the lowest $J^P = 1^+ bb\bar{b}\bar{c}$ state is 16043.2 MeV, and corresponding binding energy B_T is +303.7 MeV. Thus, the state is obviously above the lowest rearrangement meson-meson decay channel $B^*\eta_b$, and it is an unstable tetraquark state. Its variational parameters are given as $C_{11} = 12.4\text{fm}^{-2}$, $C_{22} = 21.0\text{fm}^{-2}$, and $C_{33} = 28.9\text{fm}^{-2}$. The corresponding wave function is given as:

$$|\Psi_{tot}\rangle = 0.984|F\rangle|R^s\rangle|[\phi_2\chi_4]\rangle + 0.171|F\rangle|R^s\rangle|[\phi_1\chi_3]\rangle - 0.044|F\rangle|R^s\rangle|[\phi_1\chi_2]\rangle. \quad (21)$$

Here, we notice that the mass contribution of ground state mainly come from the $|(Q_1Q_2)_0^6(Q_3Q_4)_1^6\rangle_1$ component, and other two components are negligible.

Now, let us turn our concentration to the internal contributions for this state and relative lengths between quarks. For the kinetic energy part, the state obtains 876.1 MeV, which is obviously smaller than that of the lowest meson-meson threshold $B_c\eta_b$. The actual kinetic energy of the $b - \bar{b}$ ($b - \bar{c}$) in the $J^P = 1^+ bb\bar{b}\bar{c}$ state is smaller than that inside the $\eta_b(B_c^*)$ meson. The reason can be seen in Table XI. The size of this pair is larger in the $J^P = 1^+ bb\bar{b}\bar{c}$ state than that in the meson: the distance (3,4) is 0.245 fm in this tetraquark while it is 0.148 fm in η_b .

Here, let us turn our discussion to the potential parts. The potential part of this state is far smaller than that of its lowest meson-meson threshold. Though the V^C between quark and antiquark are attractive, the V^C in the diquark and antiquark are repulsive. However, relative to the η_b and B_c mesons, the V^C in the tetraquark are less attractive. Thus, these lead to this state still have a relative large positive binding energy.

D. $cb\bar{c}\bar{b}$ state

Lastly, we investigate the $cb\bar{c}\bar{b}$ system. Similar to the $cc\bar{c}\bar{c}$ and $bb\bar{b}\bar{b}$ systems, the $cb\bar{c}\bar{b}$ system is also a pure neutral system and has a certain C-parity. Moreover, Pauli principle does not give any constraints for wave functions of the $cb\bar{c}\bar{b}$ system. Thus, comparing to other discussed tetraquark systems, the $cb\bar{c}\bar{b}$ system has more allowed states. There are four $J^{PC} = 0^{++}$ states, four $J^{PC} = 1^{+-}$ states, two $J^{PC} = 1^{++}$ states, two $J^{PC} = 2^{++}$ states in the $cb\bar{c}\bar{b}$ system.

Before discussing the numerical analysis, we compare the expectation values of the hyperfine factor of the $cb\bar{c}\bar{b}$

states with the corresponding sum of two mesons in Table XII. We note that the $\eta_c\eta_b$ decay channel is now more attractive than other channels, but the $J^{PC} = 0^{++} cb\bar{c}\bar{b}$ state is more attractive than its corresponding decay channels. Therefore, we can expect to have a stable compact tetraquarks for $J^{PC} = 0^{++} cb\bar{c}\bar{b}$ configuration. However, as we see in the Table XIII, we find that even for this state the two meson threshold lies below the tetraquark mass.

Here, we now analyse the numerical results about the $cb\bar{c}\bar{b}$ system obtained from the variational method. Here, we take the ground $J^{PC} = 0^{++} cb\bar{c}\bar{b}$ state as an example to discuss specifically, and others would have similar discussions. The mass of the lowest $J^{PC} = 0^{++} cb\bar{c}\bar{b}$ state is 12759.3 MeV, and corresponding binding energy B_T is +371.8 MeV. Thus, the state obviously has larger mass than the lowest rearrangement meson-meson decay channel $\eta_b\eta_c$, and it should be an unstable compact tetraquark state. Its variational parameters are given as $C_{11} = 11.9\text{fm}^{-2}$, $C_{22} = 11.9\text{fm}^{-2}$, and $C_{33} = 22.9\text{fm}^{-2}$. Because this state is a pure neutral state, we naturally notice that the value of C_{11} is equal to C_{22} , which means that the distance of $(b - b)$ is equal to $(\bar{b} - \bar{b})$. Our results also reflect these properties according to Table XIII. The corresponding wave function is given as:

$$|\Psi_{tot}\rangle = 0.876|F\rangle|R^s\rangle|[\phi_2\chi_2]\rangle + 0.063|F\rangle|R^s\rangle|[\phi_1\chi_2]\rangle + 0.321|F\rangle|R^s\rangle|[\phi_2\chi_3]\rangle - 0.321|F\rangle|R^s\rangle|[\phi_2\chi_4]\rangle - 0.105|F\rangle|R^s\rangle|[\phi_1\chi_3]\rangle + 0.105|F\rangle|R^s\rangle|[\phi_1\chi_4]\rangle. \quad (22)$$

Further, we find that its mass contribution of ground state mainly come from the $6\otimes\bar{6}$ component, corresponding $3\otimes\bar{3}$ component is negligible.

Here, let us now turn our discussion to the internal contribution for the ground $J^{PC} = 1^{+-} cb\bar{c}\bar{b}$ state. For the kinetic energy part, the state obtains 858.5 MeV, which is smaller than the 1001.2 MeV of the lowest meson-meson threshold $B_c\eta_b$ according to Table XIII. As for the potential part, though the V^C between quark and antiquark are attractive, the V^C in the diquark and antiquark are repulsive. However, relative to the lowest meson-meson threshold $B_c\eta_b$, the total V^C is not attractive than the $B_c\eta_b$, which leads that this state has a relatively larger mass.

We also notice that the $V^C(1,3)$, $V^C(2,3)$, $V^C(1,4)$, and $V^C(2,4)$ are absolutely same, and meanwhile the distances of (1,3), (1,4), (2,3), and (2,4) are also same. These actually reflect $\langle\Psi_{tot}|(\mathbf{R}_{1,2}\cdot\mathbf{R}_{3,4})|\Psi_{tot}\rangle = \langle\Psi_{tot}|(\mathbf{R}_{1,2}\cdot\mathbf{R}')|\Psi_{tot}\rangle = \langle\Psi_{tot}|(\mathbf{R}_{3,4}\cdot\mathbf{R}')|\Psi_{tot}\rangle = 0$. Obviously, it is unreasonable that the distance of $c\bar{c}$ is just equal to that of the $c\bar{b}$ and $b\bar{b}$. According to Sec IV of Ref. [51], we only consider single Gaussian form which the $l_1 = l_2 = l_3 = 0$ in spatial part of total wave function is not enough. These lead to the $cb\bar{c}\bar{b}$ state, which is far away from the real structures in nature. We have reason enough to believe that the $\langle\Psi_{tot}|(\mathbf{R}_{1,2}\cdot\mathbf{R}_{3,4})|\Psi_{tot}\rangle$ should not be zero. Meanwhile, considering other spatial

TABLE XII. The expectation value of the hyperfine factor for the $cb\bar{c}\bar{b}$ system and their possible decay channels. (unit: GeV^{-2})

System	$cb\bar{c}\bar{b}$ system											
J^P	0^{++}											
$\langle \sum_{i<j}^4 \frac{-\lambda_i^c \lambda_j^c \sigma_i \cdot \sigma_j}{m_i m_j} \rangle$	$\frac{-8}{3m_c m_b} - \frac{40}{3m_b m_{\bar{c}}} - \frac{20}{3m_c m_{\bar{c}}} - \frac{20}{3m_b m_{\bar{b}}}$			$\frac{-10}{\sqrt{3}m_b m_{\bar{b}}} + \frac{20}{\sqrt{3}m_b m_{\bar{c}}} - \frac{10}{\sqrt{3}m_c m_{\bar{c}}}$			$\frac{4\sqrt{2}}{m_b m_{\bar{b}}} - \frac{8\sqrt{2}}{m_b m_{\bar{c}}} + \frac{4\sqrt{2}}{m_c m_{\bar{c}}}$			$\frac{2\sqrt{6}}{m_b m_{\bar{b}}} + \frac{4\sqrt{6}}{m_b m_{\bar{c}}} + \frac{2\sqrt{6}}{m_c m_{\bar{c}}}$		
Lowest Eigenvalue	-5.50											
J^P	1^{+-}											
$\langle \sum_{i<j}^4 \frac{-\lambda_i^c \lambda_j^c \sigma_i \cdot \sigma_j}{m_i m_j} \rangle$	$\frac{2}{3} \left(\frac{-4}{m_c m_b} - \frac{10}{m_b m_{\bar{c}}} - \frac{5}{m_c m_{\bar{c}}} - \frac{5}{m_b m_{\bar{b}}} \right)$			$\frac{2\sqrt{2}}{m_b m_{\bar{b}}} - \frac{4\sqrt{2}}{m_b m_{\bar{c}}} + \frac{2\sqrt{2}}{m_c m_{\bar{c}}}$			$\frac{20}{m_b m_{\bar{b}}} - \frac{20}{m_c m_{\bar{c}}}$			$\frac{-4\sqrt{2}}{m_b m_{\bar{b}}} + \frac{4\sqrt{2}}{m_c m_{\bar{c}}}$		
Low Eigenvalue	-4.29											
J^P	1^{++}											
$\langle \sum_{i<j}^4 \frac{-\lambda_i^c \lambda_j^c \sigma_i \cdot \sigma_j}{m_i m_j} \rangle$	$\frac{2}{3} \left(\frac{-4}{m_c m_b} + \frac{5}{m_b m_{\bar{c}}} + \frac{5}{m_c m_{\bar{c}}} - \frac{10}{m_b m_{\bar{b}}} \right)$			$\frac{-2\sqrt{2}}{m_b m_{\bar{b}}} - \frac{4\sqrt{2}}{m_b m_{\bar{c}}} - \frac{2\sqrt{2}}{m_c m_{\bar{c}}}$			$\frac{2}{3} \left(\frac{4}{m_c m_b} + \frac{10}{m_b m_{\bar{c}}} - \frac{5}{m_c m_{\bar{c}}} - \frac{5}{m_b m_{\bar{b}}} \right)$			$\frac{2\sqrt{2}}{m_b m_{\bar{b}}} + \frac{4\sqrt{2}}{m_b m_{\bar{c}}} + \frac{2\sqrt{2}}{m_c m_{\bar{c}}}$		
Low Eigenvalue	-1.38											
J^P	2^{++}											
$\langle \sum_{i<j}^4 \frac{-\lambda_i^c \lambda_j^c \sigma_i \cdot \sigma_j}{m_i m_j} \rangle$	$\frac{2}{3} \left(\frac{-4}{m_c m_b} + \frac{5}{m_b m_{\bar{c}}} + \frac{5}{m_c m_{\bar{c}}} + \frac{10}{m_b m_{\bar{b}}} \right)$			$\frac{2\sqrt{2}}{m_b m_{\bar{b}}} - \frac{4\sqrt{2}}{m_b m_{\bar{c}}} + \frac{2\sqrt{2}}{m_c m_{\bar{c}}}$			$\frac{2}{3} \left(\frac{-4}{m_c m_b} + \frac{5}{m_b m_{\bar{c}}} + \frac{5}{m_c m_{\bar{c}}} + \frac{10}{m_b m_{\bar{b}}} \right)$			$\frac{2\sqrt{2}}{m_b m_{\bar{b}}} + \frac{4\sqrt{2}}{m_b m_{\bar{c}}} + \frac{2\sqrt{2}}{m_c m_{\bar{c}}}$		
Low Eigenvalue	0.97											
Decay channel	$J/\psi\Upsilon$	$J/\psi\eta_b$	$\eta_c\Upsilon$	$\eta_c\eta_b$	$B_c^*B_c^*$	$B_c^*B_c$	B_cB_c					
$\langle \frac{-\lambda_i^c \lambda_j^c \sigma_i \cdot \sigma_j}{m_i m_j} \rangle$	$\frac{16}{3m_c m_{\bar{c}}} + \frac{16}{3m_b m_{\bar{b}}}$	$\frac{16}{3m_c m_{\bar{c}}} - \frac{16}{m_b m_{\bar{b}}}$	$-\frac{16}{m_c m_{\bar{c}}} + \frac{16}{3m_b m_{\bar{b}}}$	$-\frac{16}{m_c m_{\bar{c}}} - \frac{16}{m_b m_{\bar{b}}}$	$\frac{16}{3m_c m_{\bar{c}}} + \frac{16}{3m_b m_{\bar{c}}}$	$\frac{16}{3m_c m_{\bar{c}}} - \frac{16}{m_b m_{\bar{c}}}$	$-\frac{16}{m_c m_{\bar{c}}} - \frac{16}{m_b m_{\bar{c}}}$					
Quantum number	$0^{++}, 1^{++}, 2^{++}$	1^{+-}	1^{+-}	0^{++}	$0^{++}, 1^{++}, 1^{+-}, 2^{++}$	$1^{++}, 1^{+-}$	0^{++}					
Value	1.64	0.89	-4.16	-4.91	1.04	-1.04	-3.12					

TABLE XIII. The masses, variational parameters, the internal contribution, and the relative lengths between quarks for $cb\bar{c}\bar{b}$ system, corresponding lowest meson-meson thresholds, and their differences (D_0 , D_1 , or D_2). The number is given as $i=1,2$ for the quarks, and 3,4 for the antiquarks. The masses, B_T , and contributions are in MeV unit. The relative lengths (variational parameters) are fm (fm^{-2}) unit.

System		$cb\bar{c}\bar{b}$											
J^{PC}	(i,j)	2^{++}	$\Upsilon J/\psi$	D_2	1^{+-}	$\Upsilon\eta_c$	D_1	1^{++}	$\Upsilon J/\psi$	D_1	0^{++}	$\eta_b\eta_c$	D_0
Mass/ B_T		12882.4	12561.1	321.3	12796.9	12467.4	329.5	12856.6	12561.1	295.5	12759.3	12387.5	371.8
Variational Parameters (fm^{-2})	C_{11}	11.0	12.5		11.9	49.7		11.4	12.5		12.4	15.0	
	C_{22}	11.0	49.7		11.9	15.0		11.4	49.7		12.4	57.4	
	C_{33}	21.0			22.9			21.5			23.3		
Quark Mass		14522.0	14522.0	0.0	14522.0	14522.0	0.0	14522.0	14522.0	0.0	14522.0	14522.0	0.0
Confinement Potential		-2460.7	-2926.9	466.2	-2527.1	-3000.0	472.9	-2488.0	-2926.9	438.9	-2555.2	-3082.3	527.1
Kinetic Energy		791.7	925.1	-133.4	858.5	1001.2	-142.7	818.6	925.1	-106.5	888.3	1085.5	-197.2
CS Interaction		29.5	41.0	-11.5	-41.4	-55.8	14.4	10.0	41.0	-31.0	-79.9	-137.6	57.7
V^C	(1,2)	28.0			35.6			32.0			40.0		
	(1,3)	-137.7	-164.2(J/ψ)		-158.1	-237.2(η_c)		-146.5	-164.2(J/ψ)		-167.3	-237.2(η_c)	
	(2,3)	-137.7			-158.1			-146.5			-167.3		
	(1,4)	-137.7			-158.1			-146.5			-167.3		
	(2,4)	-137.7	-796.7(Υ)		-158.1	-796.7(Υ)		-146.5	-796.7(Υ)		-167.3	-879.1(η_b)	
	(3,4)	28.0			35.6			32.0			40.0		
Total		-494.7	-960.9	466.2	-561.1	-1034.0	472.9	-522.0	-960.9	438.9	-589.2	-1116.3	527.1
Total Contribution		326.5	5.1	321.4	256.0	-88.6	344.6	306.6	5.1	301.5	219.1	-168.5	387.6
Relative Lengths (fm)	(1,2)	0.340			0.331			0.333			0.320		
	(1,3)	0.296	0.318(J/ψ)		0.289	0.290(η_c)		0.291	0.318(J/ψ)		0.280	0.290(η_c)	
	(2,3)	0.296			0.289			0.291			0.280		
	(1,4)	0.296			0.289			0.291			0.280		
	(2,4)	0.296	0.160(Υ)		0.291	0.160(Υ)		0.289	0.160(Υ)		0.280	0.148(η_b)	
	(3,4)	0.340			0.331			0.333			0.320		
(1,2)-(3,4)	0.174			0.168			0.172			0.165			

basis would reduce the corresponding to the binding energy B_T [51]. Yet these corrections would be powerless against the higher binding energy B_T of the ground $J^{PC} = 1^{+-} cb\bar{c}\bar{b}$. In conclusion, we tend to think the ground $J^{PC} = 1^{+-} cb\bar{c}\bar{b}$ state should be an unstable compact state.

V. SUMMARY

The discovery of a narrow resonance $X(6900)$ gives us strong confidence to investigate the fully heavy tetraquark system. Thus, we use the variational method systematically investigate all possible configurations for fully heavy tetraquarks within the constituent quark model.

We first estimate the theoretical values of ground fully heavy mesons. To obtain those, we need construct the total wave functions of tetraquark states, including spatial part, flavor part, color part, and spin part. Here, we construct spatial part in a simple Gaussian form. Before the discussing the numerical analysis, we also analyze the stability condition by using only the color-spin interaction. Further, we give the masses of ground states, corresponding variational parameters, specific wave functions, internal mass contributions, and relative lengths between (anti)quarks. Meanwhile, we show these results in corresponding Tables and the spatial distribution of valence quarks for the ground $J^{PC} = 0^{++} b\bar{b}\bar{b}\bar{b}$ state in Fig. 1.

For the $cc\bar{c}\bar{c}$ and $b\bar{b}\bar{b}\bar{b}$ systems, they are two pure neutral systems with definite C-parity. There are only two $J^{PC} = 0^{++}$ states, a $J^{PC} = 1^{+-}$ state, and a $J^{PC} = 2^{++}$ state, because of the Pauli Principle. Moreover, we find these states with different quantum numbers all are above the lowest thresholds, and have larger masses. Due to these states are pure neutral particles, we naturally obtain variational parameters C_{11} and C_{22} are same, correspondingly the distances of diquark and antidiquark are also same. Meanwhile, the distances between quark and antiquark are all the same following symmetry analysis of the Eqs. (15-16). Furthermore, three Jacobi coordinates are orthogonal to each other according to the Eqs. (17-19). Based on these, we take the ground $J^{PC} = 0^{++}$

$b\bar{b}\bar{b}\bar{b}$ state as an example to show the spatial distribution of four valence quarks. As for internal contribution, though the kinetic energy part is smaller than that of the $\eta_b\eta_b$ state, the V^C in η_b is much attractive relative to the ground $J^{PC} = 0^{++} b\bar{b}\bar{b}\bar{b}$ state, which is the mainly reason that this state has a larger mass than the meson-meson threshold.

Similar to $cc\bar{c}\bar{c}$ and $b\bar{b}\bar{b}\bar{b}$ systems, the $cc\bar{b}\bar{b}$ system has same number of the allowed ground states. As for the ground $J^P = 0^+$ $cc\bar{b}\bar{b}$ state, its mass contribution mainly come from $\bar{3} \otimes 3$ component. For the $cc\bar{c}\bar{b}$ and $b\bar{b}\bar{c}\bar{c}$ systems, there are more allowed states due to less symmetry restrictions. If considering the hyperfine potential only, we can expect to have a compact stable state for $J^P = 1^+$ $b\bar{b}\bar{c}\bar{c}$ configuration. However, the V^C of tetraquark are less attractive than corresponding mesons, this state still has a larger mass than the meson-meson threshold.

In the $cb\bar{c}\bar{b}$ system, these states also are pure neutral particles, and we naturally obtain their variational parameters C_{11} and C_{22} are same. There is no constraint from the Pauli principle, thus, there are four $J^{PC} = 0^{++}$ states, four $J^{PC} = 1^{+-}$ states, two $J^{PC} = 1^{++}$ states, two $J^{PC} = 2^{++}$ states. All of the $cb\bar{c}\bar{b}$ states have larger masses relative to the lowest thresholds.

Hence, we conclude that there is no compact bound ground fully heavy tetraquark state which is stable against the strong decay into two mesons within the constituent quark model. We hope our work will stimulate the interests in the fully heavy tetraquark system.

VI. ACKNOWLEDGMENTS

This work is supported by the China National Funds for Distinguished Young Scientists under Grant No. 11825503, National Key Research and Development Program of China under Contract No. 2020YFA0406400, the 111 Project under Grant No. B20063, and the National Natural Science Foundation of China under Grant No. 12047501. This project is also supported by the National Natural Science Foundation of China under Grants No. 12175091, and 11965016, and CAS Interdisciplinary Innovation Team.

-
- [1] S. K. Choi *et al.* [Belle Collaboration], Observation of a narrow charmonium - like state in exclusive $B^{+-} \rightarrow K^{+-}\pi^+\pi^- J/\psi$ decays, *Phys. Rev. Lett.* **91**, 262001 (2003).
 - [2] D. Acosta *et al.* [CDF Collaboration], Observation of the narrow state $X(3872) \rightarrow J/\psi\pi^+\pi^-$ in $\bar{p}p$ collisions at $\sqrt{s} = 1.96$ TeV, *Phys. Rev. Lett.* **93**, 072001 (2004).
 - [3] V. M. Abazov *et al.* [D0 Collaboration], Observation and properties of the $X(3872)$ decaying to $J/\psi\pi^+\pi^-$ in $p\bar{p}$ collisions at $\sqrt{s} = 1.96$ TeV, *Phys. Rev. Lett.* **93**, 162002 (2004).
 - [4] E. S. Swanson, The New heavy mesons: A Status report, *Phys. Rept.* **429**, 243 (2006).
 - [5] S. L. Zhu, New hadron states, *Int. J. Mod. Phys. E* **17** (2008) 283.
 - [6] M. B. Voloshin, Charmonium, *Prog. Part. Nucl. Phys.* **61** (2008) 455.
 - [7] N. Drenska, R. Faccini, F. Piccinini, A. Polosa, F. Renga and C. Sabelli, New Hadronic Spectroscopy, *Riv. Nuovo Cim.* **33** (2010) 633.
 - [8] A. Esposito, A. L. Guerrieri, F. Piccinini, A. Pilloni and A. D. Polosa, Four-Quark Hadrons: an Updated Review,

- Int. J. Mod. Phys. A **30** (2015) 1530002.
- [9] H. X. Chen, W. Chen, X. Liu and S. L. Zhu, The hidden-charm pentaquark and tetraquark states, Phys. Rept. **639** (2016) 1.
- [10] R. Chen, X. Liu and S. L. Zhu, Hidden-charm molecular pentaquarks and their charm-strange partners, Nucl. Phys. A **954** (2016) 406.
- [11] A. Hosaka, T. Iijima, K. Miyabayashi, Y. Sakai and S. Yasui, Exotic hadrons with heavy flavors: X, Y, Z, and related states, PTEP **2016** (2016) no.6, 062C01.
- [12] J. M. Richard, Exotic hadrons: review and perspectives, Few Body Syst. **57** (2016) no.12, 1185.
- [13] R. F. Lebed, R. E. Mitchell and E. S. Swanson, Heavy-Quark QCD Exotica, Prog. Part. Nucl. Phys. **93**, 143-194 (2017).
- [14] A. Esposito, A. Pilloni and A. D. Polosa, Multi-quark Resonances, Phys. Rept. **668**, 1-97 (2017).
- [15] A. Ali, J. S. Lange and S. Stone, Exotics: Heavy Pentaquarks and Tetraquarks, Prog. Part. Nucl. Phys. **97**, 123-198 (2017).
- [16] N. Brambilla, S. Eidelman, C. Hanhart, A. Nefediev, C. P. Shen, C. E. Thomas, A. Vairo and C. Z. Yuan, The XYZ states: experimental and theoretical status and perspectives, Phys. Rept. **873**, 1-154 (2020).
- [17] Y. R. Liu, H. X. Chen, W. Chen, X. Liu and S. L. Zhu, Pentaquark and Tetraquark states, Prog. Part. Nucl. Phys. **107** (2019), 237-320.
- [18] R. Aaij *et al.* [LHCb Collaboration], Observation of $J/\psi p$ Resonances Consistent with Pentaquark States in $\Lambda_b^0 \rightarrow J/\psi K^- p$ Decays, Phys. Rev. Lett. **115**, 072001 (2015).
- [19] R. Aaij *et al.* [LHCb Collaboration], Model-independent evidence for $J/\psi p$ contributions to $\Lambda_b^0 \rightarrow J/\psi p K^-$ decays, Phys. Rev. Lett. **117**, no. 8, 082002 (2016).
- [20] R. Aaij *et al.* [LHCb Collaboration], Observation of a narrow pentaquark state, $P_c(4312)^+$, and of two-peak structure of the $P_c(4450)^+$, Phys. Rev. Lett. **122**, no. 22, 222001 (2019).
- [21] B. Aubert *et al.* [BaBar Collaboration], Observation of a narrow meson decaying to $D_s^+ \pi^0$ at a mass of 2.32 GeV/c², Phys. Rev. Lett. **90**, 242001 (2003).
- [22] T. Barnes, F. E. Close and H. J. Lipkin, Implications of a DK molecule at 2.32-GeV, Phys. Rev. D **68** (2003), 054006.
- [23] H. Y. Cheng and W. S. Hou, B decays as spectroscopy for charmed four quark states, Phys. Lett. B **566** (2003), 193-200.
- [24] A. P. Szczepaniak, Description of the D*(s)(2320) resonance as the D pi atom, Phys. Lett. B **567** (2003), 23-26.
- [25] D. Besson *et al.* [CLEO Collaboration], Observation of a narrow resonance of mass 2.46 GeV/c² decaying to $D_s^{*+} \pi^0$ and confirmation of the $D_{sJ}^*(2317)$ state, Phys. Rev. D **68**, 032002 (2003).
- [26] S. Godfrey and N. Isgur, Mesons in a Relativized Quark Model with Chromodynamics, Phys. Rev. D **32**, 189 (1985).
- [27] A. V. Evdokimov *et al.* [SELEX Collaboration], First observation of a narrow charm-strange meson $D_{sJ}^+(2632) \rightarrow D_s^+ \eta$ and $D^0 K^+$, Phys. Rev. Lett. **93**, 242001 (2004).
- [28] V. M. Abazov *et al.* [D0], Evidence for a $B_s^0 \pi^\pm$ state, Phys. Rev. Lett. **117** (2016) no.2, 022003.
- [29] R. Aaij *et al.* [LHCb], A model-independent study of resonant structure in $B^+ \rightarrow D^+ D^- K^+$ decays, Phys. Rev. Lett. **125**, 242001 (2020).
- [30] R. Aaij *et al.* [LHCb], Amplitude analysis of the $B^+ \rightarrow D^+ D^- K^+$ decay, Phys. Rev. D **102** (2020), 112003.
- [31] X. H. Liu, M. J. Yan, H. W. Ke, G. Li and J. J. Xie, Triangle singularity as the origin of $X_0(2900)$ and $X_1(2900)$ observed in $B^+ \rightarrow D^+ D^- K^+$, Eur. Phys. J. C **80** (2020) no.12, 1178.
- [32] M. Karliner and J. L. Rosner, First exotic hadron with open heavy flavor: $cs\bar{u}\bar{d}$ tetraquark, Phys. Rev. D **102** (2020) no.9, 094016.
- [33] Z. G. Wang, Analysis of the $X_0(2900)$ as the scalar tetraquark state via the QCD sum rules, Int. J. Mod. Phys. A **35** (2020) no.30, 2050187.
- [34] Y. Huang, J. X. Lu, J. J. Xie and L. S. Geng, Strong decays of $\bar{D}^* K^*$ molecules and the newly observed $X_{0,1}$ states, Eur. Phys. J. C **80** (2020) no.10, 973.
- [35] T. J. Burns and E. S. Swanson, Kinematical cusp and resonance interpretations of the $X(2900)$, Phys. Lett. B **813** (2021), 136057.
- [36] M. W. Hu, X. Y. Lao, P. Ling and Q. Wang, $X_0(2900)$ and its heavy quark spin partners in molecular picture, Chin. Phys. C **45** (2021) no.2, 021003.
- [37] G. J. Wang, L. Meng, L. Y. Xiao, M. Oka and S. L. Zhu, Mass spectrum and strong decays of tetraquark $\bar{c}sqq$ states, Eur. Phys. J. C **81** (2021) no.2, 188.
- [38] Y. Xue, X. Jin, H. Huang and J. Ping, Tetraquarks with open charm flavor, Phys. Rev. D **103** (2021) no.5, 054010.
- [39] S. S. Agaev, K. Azizi and H. Sundu, Vector resonance $X_1(2900)$ and its structure, Nucl. Phys. A **1011** (2021), 122202.
- [40] U. Özdem and K. Azizi, Magnetic moment of the $X_1(2900)$ state in the diquark-antidiquark picture, [arXiv:2202.11466 [hep-ph]].
- [41] F. S. Yu, H. Y. Jiang, R. H. Li, C. D. Lü, W. Wang and Z. X. Zhao, Discovery Potentials of Doubly Charmed Baryons, Chin. Phys. C **42**, no.5, 051001 (2018).
- [42] R. Aaij *et al.* [LHCb Collaboration], Observation of the doubly charmed baryon Ξ_{cc}^{++} , Phys. Rev. Lett. **119**, no. 11, 112001 (2017).
- [43] S. Q. Luo, K. Chen, X. Liu, Y. R. Liu and S. L. Zhu, Exotic tetraquark states with the $qq\bar{Q}\bar{Q}$ configuration, Eur. Phys. J. C **77**, no. 10, 709 (2017).
- [44] M. Karliner and J. L. Rosner, Discovery of doubly-charmed Ξ_{cc} baryon implies a stable $(bb\bar{u}\bar{d})$ tetraquark, Phys. Rev. Lett. **119**, no. 20, 202001 (2017).
- [45] E. J. Eichten and C. Quigg, Heavy-quark symmetry implies stable heavy tetraquark mesons $Q_i Q_j \bar{q}_k \bar{q}_l$, Phys. Rev. Lett. **119**, no. 20, 202002 (2017).
- [46] A. Ali, Q. Qin and W. Wang, Discovery potential of stable and near-threshold doubly heavy tetraquarks at the LHC, Phys. Lett. B **785**, 605-609 (2018).
- [47] W. Park, S. Noh and S. H. Lee, Masses of the doubly heavy tetraquarks in a constituent quark model, Acta Phys. Polon. B **50**, 1151-1157 (2019).
- [48] T. Guo, J. Li, J. Zhao and L. He, Mass spectra of doubly heavy tetraquarks in an improved chromomagnetic interaction model, Phys. Rev. D **105** (2022) no.1, 014021.
- [49] Q. F. Lü, D. Y. Chen and Y. B. Dong, Masses of doubly heavy tetraquarks $T_{QQ'}$ in a relativized quark model, Phys. Rev. D **102** (2020) no.3, 034012.
- [50] W. Park and S. H. Lee, Color spin wave functions of heavy tetraquark states, Nucl. Phys. A **925** (2014), 161-184.
- [51] S. Noh, W. Park and S. H. Lee, The Doubly-heavy Tetraquarks $(qq'Q\bar{Q}')$ in a Constituent Quark Model

- with a Complete Set of Harmonic Oscillator Bases, Phys. Rev. D **103** (2021), 114009.
- [52] R. Aaij *et al.* [LHCb], Observation of an exotic narrow doubly charmed tetraquark, [arXiv:2109.01038].
- [53] Q. F. Lü, D. Y. Chen, Y. B. Dong and E. Santopinto, Triply-heavy tetraquarks in an extended relativized quark model, Phys. Rev. D **104** (2021) no.5, 054026.
- [54] K. Chen, X. Liu, J. Wu, Y. R. Liu and S. L. Zhu, Triply heavy tetraquark states with the $QQ\bar{Q}\bar{q}$ configuration, Eur. Phys. J. A **53**, no. 1, 5 (2017).
- [55] Y. Xing, Weak decays of triply heavy tetraquarks $b\bar{c}b\bar{q}$, Eur. Phys. J. C **80** (2020) no.1, 57.
- [56] J. F. Jiang, W. Chen and S. L. Zhu, Triply heavy $QQ\bar{Q}\bar{q}$ tetraquark states, Phys. Rev. D **96** (2017) no.9, 094022.
- [57] X. Z. Weng, W. Z. Deng and S. L. Zhu, Triply heavy tetraquark states, Phys. Rev. D **105** (2022) no.3, 034026.
- [58] J. P. Ader, J. M. Richard and P. Taxil, DO NARROW HEAVY MULTI- QUARK STATES EXIST?, Phys. Rev. D **25** (1982), 2370.
- [59] L. Heller and J. A. Tjon, On Bound States of Heavy $Q^2\bar{Q}^2$ Systems, Phys. Rev. D **32**, 755 (1985).
- [60] R. J. Lloyd and J. P. Vary, All charm tetraquarks, Phys. Rev. D **70**, 014009 (2004).
- [61] M. Karliner, S. Nussinov and J. L. Rosner, $QQ\bar{Q}\bar{Q}$ states: masses, production, and decays, Phys. Rev. D **95**, no.3, 034011 (2017).
- [62] M. N. Anwar, J. Ferretti, F. K. Guo, E. Santopinto and B. S. Zou, Spectroscopy and decays of the fully-heavy tetraquarks, Eur. Phys. J. C **78**, no.8, 647 (2018).
- [63] Y. Bai, S. Lu and J. Osborne, Beauty-full Tetraquarks, Phys. Lett. B **798**, 134930 (2019).
- [64] V. R. Debastiani and F. S. Navarra, Spectroscopy of the All-Charm Tetraquark, PoS **Hadron2017**, 238 (2018).
- [65] W. Chen, H. X. Chen, X. Liu, T. G. Steele and S. L. Zhu, Hunting for exotic doubly hidden-charm/bottom tetraquark states, Phys. Lett. B **773** (2017), 247-251.
- [66] V. Khachatryan *et al.* [CMS], Observation of $\Upsilon(1S)$ pair production in proton-proton collisions at $\sqrt{s} = 8$ TeV, JHEP **05** (2017), 013.
- [67] A. M. Sirunyan *et al.* [CMS], Measurement of the $\Upsilon(1S)$ pair production cross section and search for resonances decaying to $\Upsilon(1S)\mu^+\mu^-$ in proton-proton collisions at $\sqrt{s} = 13$ TeV, Phys. Lett. B **808** (2020), 135578.
- [68] R. Aaij *et al.* [LHCb], Search for beautiful tetraquarks in the $\Upsilon(1S)\mu^+\mu^-$ invariant-mass spectrum, JHEP **10** (2018), 086.
- [69] R. Aaij *et al.* [LHCb], Observation of structure in the J/ψ -pair mass spectrum, Sci. Bull. **65** (2020) no.23, 1983-1993.
- [70] Kai Yi on behalf of the CMS Collaboration, Recent CMS results on exotic resonance, Proceedings at ICHEP 2022, <https://agenda.infn.it/event/28874/contributions/170300/>.
- [71] Evelina Bouhova-Thacker on behalf of the ATLAS Collaboration, ATLAS results on exotic hadronic resonances, Proceedings at ICHEP 2022, <https://agenda.infn.it/event/28874/contributions/170298/>.
- [72] J. Zhao, S. Shi and P. Zhuang, Fully-heavy tetraquarks in a strongly interacting medium, Phys. Rev. D **102** (2020) no.11, 114001.
- [73] H. X. Chen, W. Chen, X. Liu and S. L. Zhu, Strong decays of fully-charm tetraquarks into di-charmonia, Sci. Bull. **65** (2020), 1994-2000.
- [74] M. S. Liu, F. X. Liu, X. H. Zhong and Q. Zhao, Full-heavy tetraquark states and their evidences in the LHCb di- J/ψ spectrum, [arXiv:2006.11952 [hep-ph]].
- [75] Q. F. Lü, D. Y. Chen and Y. B. Dong, Masses of fully heavy tetraquarks $QQ\bar{Q}\bar{Q}$ in an extended relativized quark model, Eur. Phys. J. C **80** (2020) no.9, 871.
- [76] Z. Zhao, K. Xu, A. Kaewsnod, X. Liu, A. Limphirat and Y. Yan, Study of charmoniumlike and fully-charm tetraquark spectroscopy, Phys. Rev. D **103** (2021) no.11, 116027.
- [77] F. X. Liu, M. S. Liu, X. H. Zhong and Q. Zhao, Higher mass spectra of the fully-charmed and fully-bottom tetraquarks, Phys. Rev. D **104** (2021) no.11, 116029.
- [78] H. W. Ke, X. Han, X. H. Liu and Y. L. Shi, Tetraquark state $X(6900)$ and the interaction between diquark and antidiquark, Eur. Phys. J. C **81** (2021) no.5, 427.
- [79] M. Karliner and J. L. Rosner, Interpretation of structure in the di- J/ψ spectrum, Phys. Rev. D **102** (2020) no.11, 114039.
- [80] R. N. Faustov, V. O. Galkin and E. M. Savchenko, Masses of the $QQ\bar{Q}\bar{Q}$ tetraquarks in the relativistic diquark-antidiquark picture, Phys. Rev. D **102** (2020), 114030.
- [81] B. D. Wan and C. F. Qiao, Gluonic tetracharm configuration of $X(6900)$, Phys. Lett. B **817** (2021), 136339.
- [82] C. Gong, M. C. Du, Q. Zhao, X. H. Zhong and B. Zhou, Nature of $X(6900)$ and its production mechanism at LHCb, Phys. Lett. B **824** (2022), 136794.
- [83] J. W. Zhu, X. D. Guo, R. Y. Zhang, W. G. Ma and X. Q. Li, A possible interpretation for $X(6900)$ observed in four-muon final state by LHCb – A light Higgs-like boson?, [arXiv:2011.07799 [hep-ph]].
- [84] J. Z. Wang, D. Y. Chen, X. Liu and T. Matsuki, Producing fully charm structures in the J/ψ -pair invariant mass spectrum, Phys. Rev. D **103** (2021) no.7, 071503.
- [85] J. Z. Wang and X. Liu, Improved understanding of the peaking phenomenon existing in the di- J/ψ invariant mass spectrum newly from the CMS Collaboration, [arXiv:2207.04893 [hep-ph]].
- [86] N. Santowsky and C. S. Fischer, Four-quark states with charm quarks in a two-body Bethe-Salpeter approach, Eur. Phys. J. C **82** (2022) no.4, 313.
- [87] Z. Zhuang, Y. Zhang, Y. Ma and Q. Wang, Lineshape of the compact fully heavy tetraquark, Phys. Rev. D **105** (2022) no.5, 054026.
- [88] V. R. Debastiani and F. S. Navarra, A non-relativistic model for the $[cc][\bar{c}\bar{c}]$ tetraquark, Chin. Phys. C **43** (2019) no.1, 013105.
- [89] X. Z. Weng, X. L. Chen, W. Z. Deng and S. L. Zhu, Systematics of fully heavy tetraquarks, Phys. Rev. D **103** (2021) no.3, 034001.
- [90] G. J. Wang, L. Meng and S. L. Zhu, Spectrum of the fully-heavy tetraquark state $QQ\bar{Q}'\bar{Q}'$, Phys. Rev. D **100** (2019) no.9, 096013.
- [91] C. Hughes, E. Eichten and C. T. H. Davies, Searching for beauty-fully bound tetraquarks using lattice nonrelativistic QCD, Phys. Rev. D **97** (2018) no.5, 054505.
- [92] J. M. Richard, A. Valcarce and J. Vijande, Few-body quark dynamics for doubly heavy baryons and tetraquarks, Phys. Rev. C **97** (2018) no.3, 035211.
- [93] X. Jin, Y. Xue, H. Huang and J. Ping, Full-heavy tetraquarks in constituent quark models, Eur. Phys. J. C **80**, no.11, 1083 (2020).

- [94] H. T. An, S. Q. Luo, Z. W. Liu and X. Liu, Fully heavy pentaquark states in constituent quark model, Phys. Rev. D **105** (2022) no.7, 7.
- [95] W. Park, A. Park and S. H. Lee, Dibaryons in a constituent quark model, Phys. Rev. D **92** (2015) no.1, 014037.
- [96] W. Park, A. Park and S. H. Lee, Dibaryons with two strange quarks and total spin zero in a constituent quark model, Phys. Rev. D **93** (2016) no.7, 074007.
- [97] A. Park, W. Park and S. H. Lee, Dibaryons with two strange quarks and one heavy flavor in a constituent quark model, Phys. Rev. D **94** (2016) no.5, 054027.
- [98] W. Park, A. Park, S. Cho and S. H. Lee, $P_c(4380)$ in a constituent quark model, Phys. Rev. D **95** (2017) no.5, 054027.
- [99] W. Park, S. Cho and S. H. Lee, Where is the stable pentaquark?, Phys. Rev. D **99** (2019) no.9, 094023.